TECHNIQUES FOR HIGH-PERFORMANCE DISTRIBUTED COMPUTING IN COMPUTATIONAL FLUID MECHANICS

by

Lisandro Daniel Dalcín

Dissertation submitted to the Postgraduate Department of the

FACULTAD DE INGENIERÍA Y CIENCIAS HÍDRICAS

of the

UNIVERSIDAD NACIONAL DEL LITORAL

in partial fulfillment of the requirements for the degree of

Doctor en Ingeniería - Mención Mecánica Computacional

2008

A mis padres Elda y Daniel,

a mi hermana Marianela,

a mi novia Julieta,

a la memoria de mi tia Araceli

y de mi abuela Lucrecia.

Author Legal Declaration

This dissertation have been submitted to the Postgraduate Department of the *Facultad de Ingeniería y Ciencias Hídricas* in partial fulfillment of the requirements the degree of *Doctor in Engineering - Field of Computational Mechanics* of the *Universidad Nacional del Litoral*. A copy of this document will be available at the University Library and it will be subjected to the Library's legal normative.

Some parts of the work presented in this thesis have been (or are going to be) published in the following journals: *Computer Methods in Applied Mechanics and Engineering*, *Journal of Parallel and Distributed Computing* and *Advances in Engineering Software*.

Lisandro Daniel Dalcín

Contents

List of Figures

Preface

Parallel Computing and Message Passing

Among many parallel computational models, *message-passing* has proven to be an effective one. This paradigm is specially suited for (but not limited to) distributed memory architectures. Although there are many variations, the basic concept of processes communicating through messages has been well understood from long time.

Portable message-passing parallel programming used to be a nightmare in the past. Developers of parallel applications were faced to many proprietary, incompatible and architecture-dependent message-passing libraries. Code portability was hampered by the differences between them. Fortunately, this situation definitely changed after the *Message Passing Interface* (MPI) standard specification appeared and rapidly gained acceptance.

Since its release, the MPI specification has become the leading standard for message-passing libraries in the world of parallel computers. Nowadays, MPI is being widely used in the most demanding scientific and engineering applications related to modeling, simulation, design, and signal processing. Over the last years, high performance computing has finally become an affordable resource to everyone with needs of increased computing power. The conjunction of commodity hardware and high quality open source operating systems and software packages strongly influenced the now widespread popularity of Beowulf [1] class clusters and cluster of workstations.

An important subset of scientific and engineering applications deals with problems modeled by partial differential equations on two-dimensional and

tree-dimensional domains. In those kind of applications, numerical methods are the only practical way to attack complex problems. Those methods necessarily involve a *discretization* of the governing equations at the continuum level. From this discretization process, systems of linear and nonlinear equations arise. When those systems of equations are very large, parallel processing is mandatory in order to solve them in reasonable time frames.

The popularity and availability of parallel computing resources on distributed memory architectures, together with the high degree of portability offered by the MPI specification, strongly motivated the development of general purpose, multi-platform software components tailored to efficiently solve large-scale linear and nonlinear problems.

Currently, PETSc [2] y Trilinos [3] are the most complete and advanced general purpose libraries available for supporting large-scale simulations in science and engineering. PETSc[2, 4], the *Portable Extensible Toolkit for Scientific Computation*, is a suite of state of the art algorithms and data structures for the solution of problems arising on scientific and engineering applications. It is being developed at Argonne National Laboratory, USA. PETSc is specially suited for those modeled by partial differential equations, of large-scale nature, and targeted for parallel, distributed-memory computing environments [5].

High-Level Languages for Scientific Computing

In parallel to the aforementioned trends, the popularity of some general high-level, general purpose scientific computing environments–such as MATLAB and IDL in the commercial side or Octave and Scilab in the open source side–has increased considerably. Users simply feel much more productive in such interactive environments providing tight integration of simulation and visualization. They are alleviated of low-level details associated to compilation and linking steps, memory management and input/output of the more traditional scientific programming languages like Fortran, C, and even C++.

Recently, the Python programming language [6, 7] has attracted the attention of many end-users and developers in the scientific community. Python offers a clean and simple syntax, is a very powerful language, and allows skilled

users to build their own computing environment, tailored to their specific needs and based on their favorite high-performance Fortran, C, or C++ codes. Sophisticated but easy to use and well integrated packages are available for interactive command-line work, efficient multi-dimensional array processing, 2D and 3D visualization, and other scientific computing tasks.

About This Thesis

Although a lot of progress has been made in theory as well as practice, the true costs of accessing parallel environments are still largely dominated by software. The number of end-user parallelized applications is still very small, as well as the number of people affected to their development. Engineers and scientists not specialized in programming or numerical computing, and even small and medium size software companies, hardly ever considered developing their own parallelized code. High performance computing is traditionally associated with software development using compiled languages. However, in typical applications programs, only a small part of the code is time-critical enough to require the efficiency of compiled languages. The rest of the code is generally related to memory management, error handling, input/output, and user interaction, and those are usually the most error-prone and time-consuming lines of code to write and debug in the whole development process. Interpreted high-level languages can be really advantageous for these kind of tasks.

This thesis reports the attempts to facilitate the access to high-performance parallel computing resources within a Python programming environment. The target audience are all members of the scientific and engineering community using Python on a regular basis as the supporting environment for developing applications and performing numerical simulations. The target computing platforms range from multiple-processor and/or multiple-core desktop computers, clusters of workstations or dedicated computing nodes either with standard or special network interconnects, to high-performance shared memory machines. The net result of this effort are two open source and public domain packages, MPI for Python (known in short as *mpi4py*) and PETSc for Python (known in short as *petsc4py*).

MPI for Python [8, 9, 10], is an open-source, public-domain software project that provides bindings of the *Message Passing Interface* (MPI) standard for the Python programming language. MPI for Python is a general-purpose and full-featured package targeting the development of parallel application codes in Python. Its facilities allow parallel Python programs to easily exploit multiple processors. MPI for Python employs a back-end MPI implementation, thus being immediately available on any parallel environment providing access to any MPI library.

PETSc for Python [11] is an open-source, public-domain software project that provides access to the *Portable, Extensible Toolkit for Scientific Computation* (PETSc) libraries within the Python programming language. PETSc for Python is a general-purpose and full-featured package. Its facilities allow sequential and parallel Python applications to exploit state of the art algorithms and data structures readily available in PETSc.

MPI for Python and PETSc for Python packages are fully integrated to *PETSc-FEM* [12], an MPI and PETSc based parallel, multiphysics, finite elements code. Within a parallel Python programming environment, this software infrastructure supported research activities related to the simulation of electrophoretic processes in microfluidic chips. This work is part of a multidisciplinary effort oriented to design and develop these devices in order to improve current techniques in clinical analysis and early diagnosis of cancer.

Chapter 1

Scientific Computing with Python

This chapter is an introductory one. Section 1.1 provides a general overview of the Python programing language. Section 1.2 comments some fundamental packages and development tools commonly used in the scientific community taking advantage of both the high-level features of Python and the execution performance of traditional compiled languages like C, C ++ and Fortran.

1.1 The Python Programming Language

Python [6] is a modern, easy to learn, powerful programming language. It has efficient high-level data structures and a simple but effective approach to object-oriented programming.

Python's elegant syntax, together with its interpreted nature, make it an ideal language for scripting and rapid application development. It supports modules and packages, which encourages program modularity and code reuse. Additionally, It is easily extended with new functions and data types implemented in C, C++, and Fortran. The Python interpreter and the extensive standard library are freely available in source or binary form for all major platforms, and can be freely distributed.

1.2 Tools for Scientific Computing

1.2.1 Numerical Python

NumPy [13] is an open source project providing the fundamental library needed for serious scientific computing with Python.

NumPy provides a powerful multi-dimensional array object with advanced and efficient array slicing operations to select array elements and convenient array reshaping methods. Additionally, *NumPy* contains three sub-libraries with numerical routines providing basic linear algebra operations, basic Fourier transforms and sophisticated capabilities for random number generation.

1.2.2 Scientific Tools for Python

SciPy [14] is an open source library of scientific tools for Python. It depends on the *NumPy* library, and it gathers a variety of high level science and engineering modules together as a single package.

SciPy provides modules for statistics, optimization, numerical integration, linear algebra, Fourier transforms, signal and image processing, genetic algorithms, special functions, and many more.

1.2.3 Fortran to Python Interface Generator

F2PY [15], the *Fortran to Python Interface Generator*, provides a connection between the Python and Fortran programming languages.

F2PY is a development tool for creating Python extension modules from special signature files or directly from annotated Fortran source files. The signature files, or the Fortran source files with additonal annotations included as comments, contain all the information (function names, arguments and their types, etc.) that is needed to construct convenient Python bindings to Fortran functions. The *F2PY*-generated Python extension modules enable Python codes to call those Fortran 77/90/95 routines. In addition, *F2PY* provides the required support for transparently accessing Fortran 77 *common blocks* or Fortran 90/95 *module data*.

Fortran (and specially Fortran 90 and above) is a convenient compiled language for efficiently implementing lengthy computations involving multi-dimensional arrays. Although *NumPy* provides similar and higher-level capabilities, there are situations where selected, numerically intensive parts of Python applications still requiere the efficiency of a compiled language for processing huge amounts of data in deeply-nested loops. Additionally, state of the art implementations of many commonly used algorithms are readily available and implemented in Fortran. In a Python programming environment, *F2PY* is then the tool of choice for taking advantage of the speed-up of compiled Fortran code and integrating existing Fortran libraries.

1.2.4 Simplified Wrapper and Interface Generator

SWIG [16], the *Simplified Wrapper and Interface Generator*, is an interface compiler that connects programs written in C and C++ with a variety of scripting languages.

SWIG works by taking the declarations found in C/C++ header files and using them to generate the wrapper code that scripting languages need to access the underlying C/C++ code. In addition, *SWIG* provides a variety of customization features that let developers to tailor the wrapping process to suit specific application needs.

Originally developed in 1995, *SWIG* was first used by scientists (in the Theoretical Physics Division at Los Alamos National Laboratory, USA) for building user interfaces to molecular dynamic simulation codes running on the *Connection Machine 5* supercomputer. In this environment, scientists needed to work with huge amounts of simulation data, complex hardware, and a constantly changing code base. The use of a Python scripting language interface provided a simple yet highly flexible foundation for solving these types of problems [17]. This software infrastructure nowadays supports the largest-scale molecular dynamic simulations in the world [18].

Although *SWIG* was originally developed for scientific applications, it has since evolved into a general purpose tool that is used in a wide variety of applications–in fact almost anything where C/C++ programming is involved.

Chapter 2

MPI for Python

This chapter is devoted to describing MPI for Python, an open-source, public-domain software project that provides bindings of the *Message Passing Interface* (MPI) standard for the Python programming language.

MPI for Python is a general-purpose and full-featured package targeting the development of parallel application codes in Python. It provides core facilities that allow parallel Python programs to exploit multiple processors. Sequential Python applications can also take advantages of MPI for Python by communicating through the MPI layer with external, independent parallel modules, possibly written in other languages like C++,C, or Fortran.

MPI for Python employs a back-end MPI implementation, thus being immediately available on any parallel environment providing access to any MPI library. Those environments range from multiple-processor and/or multiple-core desktop computers, clusters of workstations or dedicated computing nodes with standard or special network interconnects, to high-performance shared memory machines.

Section 2.1 presents a general description about MPI and the main concepts contained in the MPI-1 and MPI-2 specifications. Section 2.2 reviews some previous works related to MPI and Python; these works provided invaluable guidance for designing and implementing MPI for Python.

Section 2.3 describes the general design and implementation of MPI for Python through a mixed language, C-Python approach. Additionally, two

mechanisms for inter-process data communication at the Python-level are discussed. Section 2.4 presents a general overview of the many MPI concepts and functionalities accessible through MPI for Python. Additionally, a series of short, self-contained example codes with their corresponding discussions is provided. These examples show how to use MPI for Python for implementing parallel Python codes with the help of MPI.

Finally, section 2.5 presents some efficiency tests and discusses their results. Those test are focused on measuring and comparing wall clock timings of selected communication operations implemented both in C and Python.

2.1 An Overview of MPI

Among many parallel computational models, message-passing has proven to be an effective one. This paradigm is specially suited for (but not limited to) distributed memory architectures and is used in today's most demanding scientific and engineering application related to modeling, simulation, design, and signal processing.

MPI, the *Message Passing Interface*, is a standardized, portable message-passing system designed to function on a wide variety of parallel computers. The standard defines the syntax and semantics of library routines (MPI is not a programming language extension) and allows users to write portable programs in the main scientific programming languages (Fortran, C, and C++).

MPI defines a high-level abstraction for fast and portable inter-process communication [19, 20]. Applications can run in clusters of (possibly heterogeneous) workstations or dedicated nodes, (symmetric) multiprocessors machines, or even a mixture of both. MPI hides all the low-level details, like networking or shared memory management, simplifying development and maintaining portability, without sacrificing performance.

2.1.1 History

Portable message-passing parallel programming used to be a nightmare in the past because of the many incompatible options developers were faced to. Proprietary message passing libraries were available on several parallel computer systems, and were used to develop significant parallel applications. However, the code portability of those applications was hampered by the huge differences between these communication libraries. At the same time, several public-domain libraries were available. They had demonstrated that portable message-passing systems could be implemented without sacrificing performance.

In 1992, the *Message Interface Passing (MPI) Forum* [21] was born, teaming-up a group of researchers from academia and industry involving over 80 people from 40 organizations. This group undertook the effort of defining the syntax and semantics of a standard core of library routines that would be useful for a wide range of users and efficiently implementable on a wide range of parallel computing systems and environments.

The fist MPI standard specification [22], also known as MPI-1, appeared in 1994 and immediately gained widespread acceptance. After two years, a second version of the standard [23] was released. Although being completely backwards compatible, MPI-2 introduced some clarifications for features already available in MPI-1 but also many extensions and new functionalities.

The MPI specifications is nowadays the leading standard for message-passing libraries in the world of parallel computers. Implementations are available from vendors of high-performance computers and well known open source projects like MPICH [24, 25] and Open MPI [26, 27].

The MPI Forum has been dormant for nearly a decade. However, in late 2006 it reactivated for the purpose of clarifying current MPI issues, renew membership and interest, explore future opportunities, and possibly defining a new standard level. At the time of this witting, clarifications to MPI-2 are being actively discussed and new working groups are being established for generating a future MPI-3 specification.

2.1.2 Main Features of MPI

Communication Domains and Process Groups

MPI communication operations occurs within a specific communication domain through an abstraction called *communicator*. Communicators are built from *groups* of participating processes and provide a communication context for the members of those groups.

Process groups enable parallel applications to assign processing resources in sets of cooperating processes in order to perform independent work. Communicators provide a safe isolation mechanism for implementing independent parallel library routines and mixing them with user code; message passing operations within different communication domains are guaranteed to not conflict.

Processes within a group can communicate each other (including itself) through an *intracommunicator*; they can also communicate with processes within another group through an *intercommunicator*.

Intracommunicators are intended for communication between processes that are members of the same group. They have one fixed attribute: its process group. Additionally, they can have an optional, predefined attribute: a virtual *topology* (either *Cartesian* or a general *graph*) describing the logical layout of the processes in the group. This extra, optional topology attribute is useful in many ways: it can help the underlying MPI runtime system to map processes onto hardware; it simplifies the implementation of common algorithmic concepts.

Intercommunicators are intended to be used for performing communication operations between processes that are members of two disjoint groups. They provide a natural way of enabling communication between independent modules in complex, multidisciplinary applications.

Point-to-Point Communication

Point to point communication is a fundamental capability of massage passing systems. This mechanism enables the transmittal of data between a pair of processes, one side sending, the other, receiving.

MPI provides a set of send and receive functions allowing the communication of *typed* data with an associated *tag*. The type information enables the conversion of data representation from one architecture to another in the case of heterogeneous computing environments; additionally, it allows the representation of non-contiguous data layouts and user-defined datatypes, thus avoiding the overhead of (otherwise unavoidable) packing/unpacking operations. The tag information allows selectivity of messages at the receiving end.

MPI provides basic send and receive functions that are *blocking*. These functions block the caller until the data buffers involved in the communication can be safely reused by the application program.

MPI also provides *nonblocking* send and receive functions. They allow the possible overlap of communication and computation. Non-blocking communication always come in two parts: posting functions, which begin the requested operation; and test-for-completion functions, which allow to discover whether the requested operation has completed.

Collective Communication

Collective communications allow the transmittal of data between multiple processes of a group simultaneously. The syntax and semantics of collective functions is consistent with point-to-point communication. Collective functions communicate *typed* data, but messages are not paired with an associated *tag*; selectivity of messages is implied in the calling order. Additionally, collective functions come in blocking versions only.

The more commonly used collective communication operations are the following.

- Barrier synchronization across all group members.
- Global communication functions
  - Broadcast data from one member to all members of a group.
  - Gather data from all members to one member of a group.
  - Scatter data from one member to all members of a group.

- Global reduction operations such as sum, maximum, minimum, etc.

Dynamic Process Management

In the context of the MPI-1 specification, a parallel application is static; that is, no processes can be added to or deleted from a running application after it has been started. Fortunately, this limitation was addressed in MPI-2. The new specification added a process management model providing a basic interface between an application and external resources and process managers.

This MPI-2 extension can be really useful, especially for sequential applications built on top of parallel modules, or parallel applications with a client/server model. The MPI-2 process model provides a mechanism to create new processes and establish communication between them and the existing MPI application. It also provides mechanisms to establish communication between two existing MPI applications, even when one did not "start" the other.

One-Sided Operations

One-sided communications (also called *Remote Memory Access*, *RMA*) supplements the traditional two-sided, send/receive based MPI communication model with a one-sided, put/get based interface. One-sided communication that can take advantage of the capabilities of highly specialized network hardware. Additionally, this extension lowers latency and software overhead in applications written using a shared-memory-like paradigm.

The MPI specification revolves around the use of objects called *windows*; they intuitively specify regions of a process's memory that have been made available for remote read and write operations. The published memory blocks can be accessed through three functions for put (remote send), get (remote write), and accumulate (remote update or reduction) data items. A much larger number of functions support different synchronization styles; the semantics of these synchronization operations are fairly complex.

Parallel Input/Output

The POSIX [28] standard provides a model of a widely portable file system. However, the optimization needed for parallel input/output cannot be achieved with this generic interface. In order to ensure efficiency and scalability, the underlying parallel input/output system must provide a high-level interface supporting partitioning of file data among processes and a collective interface supporting complete transfers of global data structures between process memories and files. Additionally, further efficiencies can be gained via support for asynchronous input/output, strided accesses to data, and control over physical file layout on storage devices. This scenario motivated the inclusion in the MPI-2 standard of a custom interface in order to support more elaborated parallel input/output operations.

The MPI specification for parallel input/output revolves around the use objects called *files*. As defined by MPI, files are not just contiguous byte streams. Instead, they are regarded as ordered collections of *typed* data items. MPI supports sequential or random access to any integral set of these items. Furthermore, files are opened collectively by a group of processes.

The common patterns for accessing a shared file (broadcast, scatter, gather, reduction) is expressed by using user-defined datatypes. Compared to the communication patterns of point-to-point and collective communications, this approach has the advantage of added flexibility and expressiveness. Data access operations (read and write) are defined for different kinds of positioning (using explicit offsets, individual file pointers, and shared file pointers), coordination (non-collective and collective), and synchronism (blocking, nonblocking, and split collective with begin/end phases).

2.2 Related work on MPI and Python

As MPI for Python started and evolved, many ideas were borrowed from other well known open source projects related to MPI and Python.

OOMPI [29, 30] is an excellent C++ class library specification layered on top of the C bindings encapsulating MPI into a functional class hierarchy. This

library provides a flexible and intuitive interface by adding some abstractions, like *Ports* and *Messages*, which enrich and simplify the syntax.

pyMPI [31] rebuilds the Python interpreter and adds a built-in module for message passing. It permits interactive parallel runs, which are useful for learning and debugging, and provides an environment suitable for basic parallel programing. There is limited support for defining new communicators and process topologies; support for intercommunicators is absent. General Python objects can be messaged between processors; there is some support for direct communication of numeric arrays.

Pypar [32] is a rather minimal Python interface to MPI. There is no support for constructing new communicators or defining process topologies. It does not require the Python interpreter to be modified or recompiled. General Python objects of any type can be communicated. There is also good support for communicating numeric arrays and practically full MPI bandwidth can be achieved.

Scientific Python [33] provides a collection of Python modules that are useful for scientific computing. Among them, there is an interface to MPI. This interface is incomplete and does not resemble the MPI specification. However, there is good support for efficiently communicating numeric arrays.

2.3 Design and Implementation

Python has enough networking capabilities as to develop an implementation of MPI in "pure Python", i.e., without using compiled languages or depending on the availability of a third-party MPI library. The main advantage of such kind of implementation is surely portability (at least as much as Python provides); there is no need to rely on any foreign language or library. However, such an approach would have many severe limitations as to the point being considered a nonsense. Vendor-provided MPI implementations take advantage of special features of target platforms otherwise unavailable. Additionally, there are many useful and high-quality MPI-based parallel libraries; almost all them are written in compiled languages. The development of an MPI package based in calls to any available MPI implementation will sensibly ease the integration of

other parallel tools in Python. Finally, Python is really easy to extend and connect with external software components developed in compiled languages; it is expected that "wrapping" any existing MPI library would require by far less development effort than reimplementing from scratch the full MPI specification.

In subsection 2.2 some previous attempts of integrating MPI and Python were mentioned. However, all of them lack from completeness and interface conformance with the standard specification. MPI for Python provides an interface designed with focus on translating MPI syntax and semantics from the standard MPI-2 C++ bindings to Python. As syntax translation from C++ to Python is generally straightforward, any user with some knowledge of those C++ bindings should be able to use this package without need of learning a new interface specification. Of course, accessing MPI functionalities from Python necessarily requires some adjustments and enhancements in order to follow common language idioms and take better advantage of such a high-level environment.

2.3.1 Accessing MPI Functionalities

MPI for Python provides access to almost all MPI features through a two-layer, mixed language approach.

In the low-level layer, a set of extension modules written in C provide access to all functions and predefined constants in the MPI specification. Additionally, this C code implements some basic machinery for converting any MPI object between its Python representation (i.e. an instance of a specific Python class) and C representation (i.e. an opaque MPI handle). All this conversion machinery is carefully designed for interoperability; any MPI object created and managed through MPI for Python can be easily recovered at the C level and the reused for any purpose (e.g. it can be used for calling a routine in any MPI-based library accessible through a C, C++, or Fortran interface).

In the high-level layer, a module written in Python defines all class hierarchies, class methods and functions. This Python code is supported by the low-level C extension modules commented above. The final user interface

closely resembles the standard MPI-2 bindings for C++.

The mixed-language approach for implementing the high-level Python interface to MPI is exemplified in figure 2.1. In figure 2.1a, a fragment of C code shows the necessary steps in the C side: parse arguments passed from Python to C, extract the underlying MPI communicator handle form the containing Python object, make the actual call to a MPI function, and finally return back the result as a Python object. In figure 2.1b, a fragment of C code shows how the previous low-level function written in C is employed to define the method `Get_size()` of the `Comm` class providing a higher-level Python interface to MPI communicators.

```c
#include <Python.h>
#include <mpi4py.h>
/* ... */
PyObject *comm_rank(PyObject *self,
                    PyObject *args)
{
  PyObject *pycomm;
  MPI_Comm comm;
  int rank;
  PyArg_ParseTuple(args, "O", &pycomm);
  comm = PyMPIComm_AsComm(pycomm);
  MPI_Comm_rank(comm, &rank);
  return PyInt_FromLong(rank);
}
/* ... */
```

(a) C side

```python
from mpi4py import _mpi
# ...
class Comm(_mpi.Comm):
    """Communicator class"""
    # ...
    def Get_rank(self):
        """Rank of calling process"""
        return _mpi.comm_rank(self)
    # ...
# ...
```

(b) Python side

Figure 2.1: Access to `MPI_COMM_RANK` from Python.

2.3.2 Communicating Python Objects

Object Serialization

The Python standard library supports different mechanisms for data persistence. Many of them rely on disk storage, but *pickling* and *marshaling* can also work with memory buffers.

The `pickle` (slower, written in pure Python) and `cPickle` (faster, written in C) modules provide user-extensible facilities to serialize general Python objects using ASCII or binary formats. The `marshal` module provides facilities

to serialize built-in Python objects using a binary format specific to Python, but independent of machine architecture issues.

MPI for Python can communicate any general or built-in Python object taking advantage of the features provided by `cPickle` and `marshal` modules. Their functionalities are wrapped in two classes, `Pickle` and `Marshal`, defining `dump()` and `load()` methods. These are simple extensions, being completely unobtrusive for user-defined classes to participate (they actually use the standard pickle protocol), but carefully optimized for serialization of Python objects on memory streams.

This approach is also fully extensible; that is, users are allowed to define new, custom serializers implementing the generic `dump()/load()` interface. Any provided or user-defined serializer can be attached to communicator instances. They will be routinely used to build binary representations of objects to communicate (at sending processes), and restoring them back (at receiving processes).

Memory Buffers

Although simple and general, the serialization approach (i.e. *pickling* and *unpickling*) previously discussed imposes important overheads in memory as well as processor usage, especially in the scenario of objects with large memory footprints being communicated. The reasons for this are simple. Pickling general Python objects, ranging from primitive or container built-in types to user-defined classes, necessarily requires computer resources. Processing is needed for dispatching the appropriate serialization method (that depends on the type of the object) and doing the actual packing. Additional memory is always needed, and if its total amount in not known *a priori*, many reallocations can occur. Indeed, in the case of large numeric arrays, this is certainly unacceptable and precludes communication of objects occupying half or more of the available memory resources.

MPI for Python supports direct communication of any object exporting the single-segment buffer interface. This interface is a standard Python mechanism provided by some types (e.g. strings and numeric arrays), allowing access in the

C side to a contiguous memory buffer (i.e. address and length) containing the relevant data. This feature, in conjunction with the capability of constructing user-defined MPI datatypes describing complicated memory layouts, enables the implementation of many algorithms involving multidimensional numeric arrays (e.g. image processing, fast Fourier transforms, finite difference schemes on structured Cartesian grids) directly in Python, with negligible overhead, and almost as fast as compiled Fortran, C, or C++ codes.

2.4 Using MPI for Python

This section presents a general overview and some examples of many MPI concepts and functionalities readily available in MPI for Python. Discussed features range from classical MPI-1 message-passing communication operations to and more advances MPI-2 operations like dynamic process management, one-sided communication, and parallel input/output.

2.4.1 Classical Message-Passing Communication

Communicators

In MPI for Python, `Comm` is the base class of communicators. Communicator size and calling process rank can be respectively obtained with methods `Get_size()` and `Get_rank()`.

The `Intracomm` and `Intercomm` classes are derived from the `Comm` class. The `Is_inter()` method (and `Is_intra()`, provided for convenience, it is not part of the MPI specification) is defined for communicator objects and can be used to determine the particular communicator class.

The two predefined intracommunicator instances are available: `COMM_WORLD` and `COMM_SELF` (or `WORLD` and `SELF`, they are just aliases provided for convenience). From them, new communicators can be created as needed.

New communicator instances can be obtained with the `Clone()` method of `Comm` objects, the `Dup()` and `Split()` methods of `Intracomm` and `Intercomm` objects, and methods `Create_intercomm()` and `Merge()` of `Intracomm` and `Intercomm` objects respectively.

Virtual topologies (`Cartcomm` and `Graphcomm` classes, both being a specialization of `Intracomm` class) are fully supported. New instances can be obtained from intracommunicator instances with factory methods `Create_cart()` and `Create_graph()` of `Intracomm` class.

The associated process group can be retrieved from a communicator by calling the `Get_group()` method, which returns am instance of the `Group` class. Set operations with `Group` objects like like `Union()`, `Intersect()` and `Difference()` are fully supported, as well as the creation of new communicators from these groups.

Blocking Point-to-Point Communications

The `Send()`, `Recv()` and `Sendrecv()` methods of communicator objects provide support for blocking point-to-point communications within `Intracomm` and `Intercomm` instances. These methods can communicate either general Python objects or raw memory buffers.

Figure 2.2 shows an example of high-level communication of Python objects. Process zero creates and next sends a Python dictionary to all other processes; the other processes just issue a receive call for getting the sent object. MPI for Python automatically serializes (at sending process) and deserializes (at receiving processes) Python objects as needed.

```
from mpi4py import MPI

comm = MPI.COMM_WORLD
size = comm.Get_size()
rank = comm.Get_rank()

if rank == 0:
    # create a Python 'dict' object
    data = {'key1' : [7, 2.72, 2+3j],
            'key2' : ('abc', 'xyz')}
    # send the object to all other processes
    for i in range(1, size):
        comm.Send(data, dest=i, tag=3)
else:
    # receive a Python object from process
    data = comm.Recv(None, source=0, tag=3)
    # the received object should be a 'dict'
    assert type(data) is dict
```

Figure 2.2: Sending and Receiving general Python objects.

Additional examples of blocking point-to-point communication operations

can be found in section 2.5. Those examples show how MPI for Python can efficiently communicate *NumPy* arrays by directly using their exposed memory buffers, thus avoiding the overhead of serialization and deserialization steps.

Nonblocking Point-to-Point Communications

On many systems, performance can be significantly increased by overlapping communication and computation. This is particularly true on systems where communication can be executed autonomously by an intelligent, dedicated communication controller. Nonblocking communication is a mechanism provided by MPI in order to support such overlap.

The inherently asynchronous nature of nonblocking communications currently imposes some restrictions in what can be communicated through MPI for Python. Communication of memory buffers, as described in section 2.3.2 is fully supported. However, communication of general Python objects using serialization, as described in section 2.3.2, is possible but not transparent since objects must be explicitly serialized at sending processes, while receiving processes must first provide a memory buffer large enough to hold the incoming message and next recover the original object.

The `Isend()` and `Irecv()` methods of the `Comm` class initiate a send and receive operation respectively. These methods return a `Request` instance, uniquely identifying the started operation. Its completion can be managed using the `Test()`, `Wait()`, and `Cancel()` methods of the `Request` class. The management of `Request` objects and associated memory buffers involved in communication requires a careful, rather low-level coordination. Users must ensure that objects exposing their memory buffers are not accessed at the Python level while they are involved in nonblocking message-passing operations.

Often a communication with the same argument list is repeatedly executed within an inner loop. In such cases, communication can be further optimized by using persistent communication, a particular case of nonblocking communication allowing the reduction of the overhead between processes and communication controllers. Furthermore , this kind of optimization can also

alleviate the extra call overheads associated to interpreted, dynamic languages like Python. The `Send_init()` and `Recv_init()` methods of the `Comm` class create a persistent request for a send and receive operation respectively. These methods return an instance of the `Prequest` class, a subclass of the `Request` class. The actual communication can be effectively started using the `Start()` method, and its completion can be managed as previously described.

Figure 2.3 shows a mixture of blocking and nonblocking point-to-point communication involving three processes. Process zero and two send data to process three using standard, blocking send calls; the messages have the same length but they are tagged with different values. Process three issues two nonblocking receive calls specifying a wildcard value for the source process, but explicitly selecting messages by their tag values; the data is received in a two-dimensional array with two rows and enough columns to hold each message. The nonblocking receive calls at process three return request objects, they are next waited for completion. While messages are in transit (between the post-receive calls and the call waiting for completion), process three can use its computing resources for any other local task, thus effectively overlapping computation with communication. The outcome of this message interchange is the following: process three receives the message sent from process zero in the second row of the local data array; the the message sent from process one is received in the fist row of the local data array.

Collective Communications

The `Bcast()`, `Scatter()`, `Gather()`, `Allgather()` and `Alltoall()` methods of `Intracomm` instances provide support for collective communications. Those methods can communicate either general Python objects or raw memory buffers. The vector variants (which can communicate different amounts of data at each process) `Scatterv()`, `Gatherv()`, `Allgatherv()` and `Alltoallv()` are also supported, they can only communicate objects exposing raw memory buffers.

Global reduction operations are accessible through the `Reduce()`, `Allreduce()`, `Scan()` and `Exscan()` methods. All the predefined (i.e., `SUM`,

```
from mpi4py import MPI
import numpy

comm = MPI.COMM_WORLD
size = comm.Get_size()
rank = comm.Get_rank()

assert size == 3, 'run me in three processes'

if rank == 0:
    # send a thousand integers to process two
    data = numpy.ones(1000, dtype='i')
    comm.Send([data, MPI.INT], dest=2, tag=35)
elif rank == 1:
    # send a thousand integers to process two
    data = numpy.arange(1000, dtype='i')
    comm.Send([data, MPI.INT], dest=2, tag=46)
else:
    # create empty integer 2d array with two rows and
    # a thousand columns to hold received data
    data = numpy.empty([2, 1000], dtype='i')
    # post for receive 1000 integers with message tag 46
    # from any source and store it in the firt row
    req1 = comm.Irecv([data[0, :], MPI.INT],
                      source=MPI.ANY_SOURCE, tag=46)
    # post for receive 1000 integers with message tag 35
    # from any source and store it in the second row
    req2 = comm.Irecv([data[1, :], MPI.INT],
                      source=MPI.ANY_SOURCE, tag=35)
    # >> you could do other useful computations
    # >> here while the messages are in transit !!!
    MPI.Request.Waitall([req1, req2])
    # >> now you can safely use the received data;
    # >> for example, the fist five columns of
    # >> data array can be printed to 'stdout'
    print data[:, 0:5]
```

Figure 2.3: Nonblocking Communication of Array Data.

`PROD`, `MAX`, etc.) and even user-defined reduction operations can be applied to general Python objects (however, the actual required computations are performed sequentially at some process). Reduction operations on memory buffers are supported, but in this case only the predefined MPI operations can be used.

Figure 2.4 shows an example of high-level communication of Python objects. A Python dictionary created a process zero, next it is collectively broadcast to all other processes within a communicator.

An additional example of collective communication is shown in figure 2.5. In this case, *NumPy* arrays are communicated by using their exposed memory buffers, thus avoiding the overhead of serialization/deserialization steps. This example implements a parallel dense matrix-vector product $y = Ax$. For the

```
from mpi4py import MPI

comm = MPI.COMM_WORLD
rank = comm.Get_rank()

# create a Python 'dict' object,
# but only at process zero
if rank == 0:
    data = {'key1' : [7, 2.72, 2+3j],
            'key2' : ( 'abc', 'xyz')}
else:
    data = None
# broadcast Python object created at
# process zero to all other processes
data = comm.Bcast(data, root=0)
# now all processes should have a 'dict'
assert type(data) is dict
```

Figure 2.4: Broadcasting general Python objects.

sake of simplicity, the input global matrix A is assumed to be square and block-distributed by rows within a group of processes with p members, each process owning m consecutive rows from a total of mp global rows. The input vector x and output vector y also have block-distributed entries in compatibility with the row distribution of matrix A. The final implementation is straightforward. The global concatenation of input vector x is obtained at all processes through a *gather-to-all* collective operation, a matrix-vector product with the local portion of A is performed, and the readily distributed output vector y is finally obtained.

```
from mpi4py import MPI
import numpy

def matvec(comm, A, x):
    "A x  -> y"
    m = len(x)
    p = comm.Get_size()
    xg = numpy.zeros(m*p, dtype='d')
    comm.Allgather([x,  MPI.DOUBLE],
                   [xg, MPI.DOUBLE])
    y = numpy.dot(A, xg)
    return y
```

Figure 2.5: Distributed Dense Matrix-Vector Product.

2.4.2 Dynamic Process Management

In MPI for Python, new independent processes groups can be created by calling the `Spawn()` method within an intracommunicator (i.e., an `Intracomm` instance). This call returns a new intercommunicator (i.e., an `Intercomm` instance) at the parent process group. The child process group can retrieve the matching intercommunicator by calling the `Get_parent()` method defined in the `Comm` class. At each side, the new intercommunicator can be used to perform point to point and collective communications between the parent and child groups of processes.

Alternatively, disjoint groups of processes can establish communication using a client/server approach. Any server application must first call the `Open_port()` function to open a "port" and the `Publish_name()` function to publish a provided "service", and next call the `Accept()` method within an `Intracomm` instance. Any client applications can first find a published "service" by calling the `Lookup_name()` function, which returns the "port" where a server can be contacted; and next call the `Connect()` method within an `Intracomm` instance. Both `Accept()` and `Connect()` methods return an `Intercomm` instance. When connection between client/server processes is no longer needed, all of them must cooperatively call the `Disconnect()` method of the `Comm` class. Additionally, server applications should release resources by calling the `Unpublish_name()` and `Close_port()` functions.

As an example, figures 2.6 and 2.7 show a Python and a C++ implementation of a master/worker approach for approximately computing the number π in parallel through a simple numerical quadrature applied to the definite integral $\int_0^1 4(1+x^2)^{-1}dx$.

The codes on the left (figures 2.6a and 2.7a) implement "master", sequential applications. These master applications create a new group of independent processes and communicate with them by sending (through a *broadcast* operation) and receiving (through a *reduce* operation) data. The codes on the right (figures 2.6b and 2.7b) implement "worker", parallel applications. These worker applications are in charge of receiving input data from the master (through a matching *broadcast* operation), making the actual computations,

and sending back the results (through a matching *reduce* operation).

A careful look at figures 2.6a and 2.7a reveals that, for each implementation language, the sequential master application spawns the worker application implemented in the matching language. However, this setup can be easily changed: the master application written in Python can stead spawn the worker application written in C++; the master application written in C++ can instead spawn the worker application written in Python. Thus MPI for Python and its support for dynamic process management automatically provides full interoperability with other codes using a master/worker (or client/server) model, regardless of their specific implementation languages being C, C++, or Fortran.

```
#! /usr/local/bin/python
# file: master.py
from mpi4py import MPI
from numpy import array
N  = array(100, 'i')
PI = array(0.0, 'd')
cmd = 'worker.py'
args = []
master = MPI.COMM_SELF
worker = master.Spawn(cmd, args, 5)
worker.Bcast([N,MPI.INT], root=MPI.ROOT)
sbuf = None
rbuf = [PI, MPI.DOUBLE]
worker.Reduce(sbuf, rbuf,
              op=MPI.SUM,
              root=MPI.ROOT)
worker.Disconnect()
print PI
```

(a) Master Python code

```
#! /usr/local/bin/python
# file: worker.py
from mpi4py import MPI
from numpy import array
N  = array(0, 'i')
PI = array(0, 'd')
master = MPI.Comm.Get_parent()
np = master.Get_size()
ip = master.Get_rank()
master.Bcast([N, MPI.INT], root=0)
h = 1.0 / N
s = 0.0
for i in xrange(ip, N, np):
    x = h * (i + 0.5)
    s += 4.0 / (1.0 + x**2)
PI[...] = s * h
sbuf = [PI, MPI.DOUBLE]
rbuf = None
master.Reduce(sbuf, rbuf,
              op=MPI.SUM,
              root=0)
master.Disconnect()
```

(b) Worker Python code

Figure 2.6: Computing π with a Master/Worker Model in Python.

2.4.3 One-sided Operations

In MPI for Python, one-sided operations are available by using instances of the `Win` class. New window objects are created by calling the `Create()` method at all processes within a communicator and specifying a memory buffer (i.e.,

```
// file: master.cxx
// make: mpicxx master.cxx -o master
#include <mpi.h>
#include <iostream>
int main()
{
  MPI::Init();
  int N = 100;
  double PI = 0.0;
  const char cmd[] = "worker";
  const char* args[] = { 0 };
  MPI::Intracomm master =
    MPI::COMM_SELF;
  MPI::Intercomm worker =
    master.Spawn(cmd, args, 5,
                 MPI_INFO_NULL, 0,
                 MPI_ERRCODES_IGNORE);
  worker.Bcast(&N, 1, MPI_INT, MPI_ROOT);
  worker.Reduce(MPI_BOTTOM, &PI,
                1, MPI_DOUBLE,
                MPI_SUM, MPI_ROOT);
  worker.Disconnect();
  std::cout << PI << std::endl;
  MPI::Finalize();
  return 0;
}
```

(a) Master C++ code

```
// file: worker.cxx
// make: mpicxx worker.cxx -o worker
#include <mpi.h>
int main()
{
  MPI::Init();
  int N;
  double PI;
  MPI::Intercomm master =
    MPI::Comm::Get_parent();
  int np = master.Get_size();
  int ip = master.Get_rank();
  master.Bcast(&N, 1, MPI_INT, 0);
  double h = 1.0 / (double) N;
  double s = 0.0;
  for (int i=ip; i<N; i+=np) {
    double x = h * (i + 0.5);
    s += 4.0 / (1.0 + x*x);
  }
  PI = s * h;
  master.Reduce(&PI, MPI_BOTTOM,
                1, MPI_DOUBLE,
                MPI_SUM, 0);
  master.Disconnect();
  MPI::Finalize();
  return 0;
}
```

(b) Worker C++ code

Figure 2.7: Computing π with a Master/Worker Model in C++.

a base address and length). When a window instance is no longer needed, the `Free()` method should be called.

The three one-sided MPI operations for remote write, read and reduction are available through calling the methods `Put()`, `Get()`, and `Accumulate()` respectively within a `Win` instance. These methods need an integer rank identifying the target process and an integer offset relative the base address of the remote memory block being accessed.

The one-sided operations read, write, and reduction are implicitly nonblocking, and must be synchronized by using two primary modes. Active target synchronization requires the origin process to call the `Start()`/`Complete()` methods at the origin process, and target process cooperates by calling the `Post()`/`Wait()` methods. There is also a collective variant provided by the `Fence()` method. Passive target synchronization is more lenient, only the origin process calls the `Lock()`/`Unlock()` methods. Locks are used to protect remote accesses to the locked remote window and to protect local load/store

accesses to a locked local window.

As an example, figures 2.8 and 2.9 show two possible implementations of a parallel indirect assignment $B = A(I)$, were A and B are two one-dimensional, double precision floating point arrays and I is an integer permutation array. For the sake of simplicity, A, B, and I are assumed to have the same block-distribution with m local entries in p processes within a communicator.

In both implementations, a new window object is created by calling the `Create()` method of the `Win` class. The window is constructed to make available the memory block of each local input array A at a group of processes implicitly defined by a communicator. Additionally, a displacement unit equal to the *extent* of the `DOUBLE` predefined datatype is specified; this extent is computed from the *lower bound* and *upper bound* obtained through the method `Get_extent()` of the `Datatype` class. The memory block of local output array B is the destination of remote `Get()` operations; they are issued between a couple of calls to the collective, barrier-like synchronization operation on the window object through the `Fence()` method.

The simpler version shown in figure 2.8 is a pure-Python implementation. It just computes the target process and the remote entry index for each needed local entry, and issues a `Get()` call in order to obtain the corresponding local value. As there are m remote memory accesses, this version is expected to be slow for large arrays.

The more efficient but complex version shown in figure 2.9 is a mixed Python-Fortran implementation. It requires only p remote memory accesses, thus being expected to be faster than the previous version for larger arrays.

The auxiliary Fortran code shown in figure 2.9a implements a helper routine in charge of computing the index mapping associating needed local entries to remote entries at each process. This routine is made available to Python by using *F2PY* interface generator.

The core Python code shown in figure 2.9b employs the output of the helper Fortran routine for constructing user-defined MPI datatypes. Those datatypes are created through the constructor method `Create_indexed_block()` of the `Datatype` class; they contain the required information in order to access local and remote array entries. Finally, those used-defined datatypes are employed

```
from mpi4py import MPI

def permute(comm, A, I, B):
    """B <- A[I]"""
    p = comm.Get_size() # number of processors
    m = len(I) # local block size
    # create window with local memory block
    lb, ub = MPI.DOUBLE.Get_extent()
    win = MPI.Win.Create(A, ub-lb, None, comm)
    # this part does the assignment itself
    win.Fence()
    for i in range(m): # local entry index
        b = B[i,...] # local entry buffer
        j = I[i] // m # remote processor
        k = I[i]  % m # remote entry index
        origin = (b, 1, MPI.DOUBLE)
        target = (k, 1, MPI.DOUBLE)
        win.Get(origin, j, target)
    win.Fence()
    # destroy the created window
    win.Free()
```

Figure 2.8: Permutation of Block-Distributed 1D Arrays (slow version).

for issuing the required p remote memory `Get()` operations.

2.4.4 Parallel Input/Output Operations

In MPI for Python, all MPI input/output operations are performed through instances of the `File` class. File handles are obtained by calling method `Open()` at all processes within a communicator and providing a file name and the intended access mode. After use, they must be closed by calling the `Close()` method. Files even can be deleted by calling method `Delete()`.

After creation, files are typically associated with a per-process *view*. The view defines the current set of data visible and accessible from an open file as an ordered set of elementary datatypes. This data layout can be set and queried with the `Set_view()` and `Get_view()` methods respectively.

Actual input/output operations are achieved by many methods combining read and write calls with different behavior regarding positioning, coordination, and synchronism. Summing up, MPI for Python provides the thirty (30) different methods defined in MPI-2 for reading from or writing to files using explicit offsets or file pointers (individual or shared), in blocking or nonblocking and collective or noncollective versions.

As an example, figure 2.10 show a pure-Python implementation of a routine

```python
from mpi4py import MPI
from pmaplib import mkidx

def permute(comm, A, I, B):
    """B <- A[I]"""
    p = comm.Get_size()
    # compute origin and target indices
    dist, oindex, tindex = mkidx(p, I)
    # create origin and target datatypes
    abtype = MPI.DOUBLE # base datatype
    mktype = abtype.Create_indexed_block
    otype, ttype = [], []
    for i in range(p):
        j, k = dist[i], dist[i+1]
        ot = mktype(1, oindex[j:k])
        tt = mktype(1, tindex[j:k])
        ot.Commit(); otype.append(ot)
        tt.Commit(); ttype.append(tt)
    # create a window
    lb, ub = MPI.DOUBLE.Get_extent()
    win = MPI.Win.Create(A, ub-lb,
                         None, comm)
    # do the assignment itself
    win.Fence()
    for i in range(p):
        origin = (B, 1, otype[i])
        target = (0, 1, ttype[i])
        win.Get(origin, i, target)
    win.Fence()
    # destroy the created MPI objects
    for ot in otype: ot.Free()
    for tt in ttype: tt.Free()
    win.Free()
```

(a) Core Python code

```fortran
! to build a Python module, use this:
! $$ f2py -m pmaplib -c pmaplib.f90
SUBROUTINE mkidx(p, m, perm, &
                 dist, oindex, tindex)
!f2py intent(hide)   :: m
!f2py depend(perm)   :: m = len(perm)
INTEGER, INTENT(IN)  :: p, m, perm(m)
INTEGER, INTENT(OUT) :: dist(p+1)
INTEGER, INTENT(OUT) :: oindex(m)
INTEGER, INTENT(OUT) :: tindex(m)
INTEGER i, j, k, counter(p)
! compute number of entries
! to be received from each process
counter(:) = 0
DO i=1,m
   j = perm(i)/m+1
   counter(j) = counter(j)+1
END DO
dist(1) = 0
DO i=1,p
   dist(i+1) = dist(i) + counter(i)
END DO
! compute origin and target
! indices of entries;  entry 'i' at
! current process is received
! from location 'k' at process 'j'.
counter(:) = 0
DO i=1,m
   j = perm(i)/m+1
   counter(j) = counter(j)+1
   oindex(dist(j) + counter(j)) = i-1
   k = MOD(perm(i),m)
   tindex(dist(j) + counter(j)) = k
END DO
END SUBROUTINE mkidx
```

(b) Auxiliary Fortran code

Figure 2.9: Permutation of Block-Distributed 1D Arrays (fast version).

for reading and writing distributed 2D arrays. For the sake of simplicity, arrays are assumed to have a block-distribution by rows on p processes with m local rows at each process, $m \cdot p$ global rows and M local and global columns in a standard C memory layout (i.e. row-major ordering).

A key point in simplifying the implementation of this routine is the usage of the MPI-2 subarray datatype constructor, available in MPI for Python through the method `Create_subarray()` of the `Datatype` class. This constructor creates a new used-defined datatype by specifying at each process the owned section of the global array. This datatype is then employed for defining the local file view. After setting the file view, the actual data can be retrieved from or dumped to the file by calling the blocking, collective operations pro-

vided by the `Read_all()` or `Write_all()` methods.

```
from mpi4py import MPI

def arrayio(op, A, atype, filename, comm):
    # create datatype for setting the file view on
    # this process; global array has dimensions (M,M),
    # all local arrays have local dimension (m,M).
    rank = comm.Get_rank()
    m, M = A.shape
    sizes = [M, M] # global array shape
    subsizes = [m, M] # local subarray shape
    starts = [m*rank, 0] # start of section here
    order = MPI.ORDER_C # ie. row major order
    mktype = atype.Create_subarray # constructor
    view = mktype(sizes, subsizes, starts, order)
    # open file for reading or writing,
    # additionally, set file view datatype
    if op == 'r':
        mode = MPI.MODE_RDONLY
    elif op == 'w':
        mode = MPI.MODE_WRONLY | MPI.MODE_CREATE
    fh = MPI.File.Open(comm, filename, mode)
    fh.Set_view(etype=atype, filetype=view)
    # read or write data
    if op == 'r':
        fh.Read_all([A, atype])
    elif op == 'w':
        fh.Write_all([A, atype])
    # close opened file, free view datatype
    fh.Close()
    view.Free()

def read(A, atype, filename, comm):
    arrayio('r', A, atype, filename, comm)

def write(A, atype, filename, comm):
    arrayio('w', A, atype, filename, comm)
```

Figure 2.10: Input/Output of Block-Distributed 2D Arrays.

2.5 Efficiency Tests

Some efficiency tests were run on the Beowulf class cluster *Aquiles* [34]. Its hardware consists of eighty disk-less single processor computing nodes with Intel Pentium 4 Prescott 3.0GHz 2MB cache processors, Intel Desktop Board D915PGN motherboards, Kingston Value RAM 2GB DDR 400MHz memory, and 3Com 2000ct Gigabit LAN network cards, interconnected with a 3Com SuperStack 3 Switch 3870 48-ports Gigabit Ethernet.

MPI for Python was built on a *Linux 2.6.17* box using *GCC 3.4.6* compiler

with *Python 2.5.1*. The chosen MPI implementation was *MPICH2 1.0.5p4*. Communications between processes involved numeric arrays, they were provided by *NumPy 1.0.3*.

2.5.1 Measuring Overhead in Message Passing Operations

The first test consisted in blocking send and receive operations (`MPI_SEND` and `MPI_RECV`) between a pair of nodes. Messages were numeric arrays of double precision (64 bits) floating-point values. The two supported communications mechanisms, object serialization (see section 2.3.2) and memory buffers (see section 2.3.2), were compared against compiled C code. A basic implementation of this test using MPI for Python with direct communication of memory buffers (translation to C or C++ is straightforward) is shown in figure 2.11. Results are shown in figure 2.14. Throughput is computed as $2S/\Delta t$, where S is the basic message size (in megabytes), and Δt is the measured wall-clock time. Clearly, the overhead introduced by object serialization degrades overall efficiency; the maximum throughput in Python is about 60% of the one in C. However, the direct communication of memory buffers introduces a negligible overhead for medium-sized to long arrays.

The second test was a variation of the previous one. The interchange of messages consisted in a bidirectional send/receive operation (`MPI_SENDRECV`). A basic implementation of this test using MPI for Python with direct communication of memory buffers (translation to C or C++ is straightforward) is shown in figure 2.12. Results are shown in figure 2.15. In comparison to the previous test, the overhead introduced by object serialization is lower (the maximum throughput in Python is about 75% of the one in C) and the overhead communicating memory buffers is similar (and again, it is negligible for medium-sized to long arrays).

The third test consisted in an all-to-all collective operation (`MPI_ALLTOALL`) on sixteen nodes. As in previous tests, messages were numeric arrays of double precision floating-point values. A basic implementation of this test using MPI for Python with direct communication of memory buffers (translation to C

or C++ is straightforward) is shown in figure 2.13. Results are shown in figure 2.16. Throughput is computed as $2(N-1)S/\Delta t$, where N is the number of nodes, S is the basic message size (in megabytes), and Δt is the measured wall-clock time. The overhead introduced by object serialization is notably more significant than in previous tests; the maximum throughput in Python is about 40% of the one in C. However, the overhead communicating memory buffers is always below 1.5%.

Finally, some remarks are worth to be done on the implementation of the previous tests and the obtained efficiency results.

The snippets of code shown in the discussion above were included just for reference. For each test case, the actual implementation took into account memory preallocation (in order to avoid paging effects) and parallel synchronization (in order to avoid asynchronous skew in the start-up phase). Timings were measured many times inside a loop over each single run and the minimum were taken.

All tests involved communications of one-dimensional, contiguous *NumPy* arrays. For those kind of objects, serialization and deserialization with the *pickle* protocol is implemented quite efficiently. The serialization step is accomplished with memory copying into a raw string object. The deserialization step reuses this raw string object, thus saving from extra memory allocations and copies. These optimizations are possible because the total amount of memory required for serialization is known in advance and all items have a common data type corresponding to a C primitive type. For more general Python objects, the serialization approach is expected to achieve lower performance than the one previously reported.

```
from mpi4py import MPI
from numpy import empty, float64
comm = MPI.COMM_WORLD
rank = comm.Get_rank()
array1 = empty(2**16, dtype=float64)
array2 = empty(2**16, dtype=float64)
wt = MPI.Wtime()
if rank == 0:
    comm.Send([array1, MPI.DOUBLE], 1, tag=0)
    comm.Recv([array2, MPI.DOUBLE], 1, tag=0)
elif rank == 1:
    comm.Recv([array2, MPI.DOUBLE], 0, tag=0)
    comm.Send([array1, MPI.DOUBLE], 0, tag=0)
wt = MPI.Wtime() - wt
```

Figure 2.11: Python code for timing a blocking Send and Receive.

```
from mpi4py import MPI
from numpy import empty, float64
comm = MPI.COMM_WORLD
rank = comm.Get_rank()
array1 = empty(2**16, dtype=float64)
array2 = empty(2**16, dtype=float64)
wt = MPI.Wtime()
if rank == 0:
    comm.Sendrecv([array1, MPI.DOUBLE], 1, 0,
                  [array2, MPI.DOUBLE], 1, 0)
elif rank == 1:
    comm.Sendrecv([array1, MPI.DOUBLE], 0, 0,
                  [array2, MPI.DOUBLE], 0, 0)
wt = MPI.Wtime() - wt
```

Figure 2.12: Python code for timing a bidirectional Send/Receive.

```
from mpi4py import MPI
from numpy import empty, float64
comm = MPI.COMM_WORLD
size = comm.Get_size()
array1 = empty([size, 2**16], dtype=float64)
array2 = empty([size, 2**16], dtype=float64)
wt = MPI.Wtime()
comm.Alltoall([array1, MPI.DOUBLE],
              [array2, MPI.DOUBLE])
wt = MPI.Wtime() - wt
```

Figure 2.13: Python code for timing All-To-All.

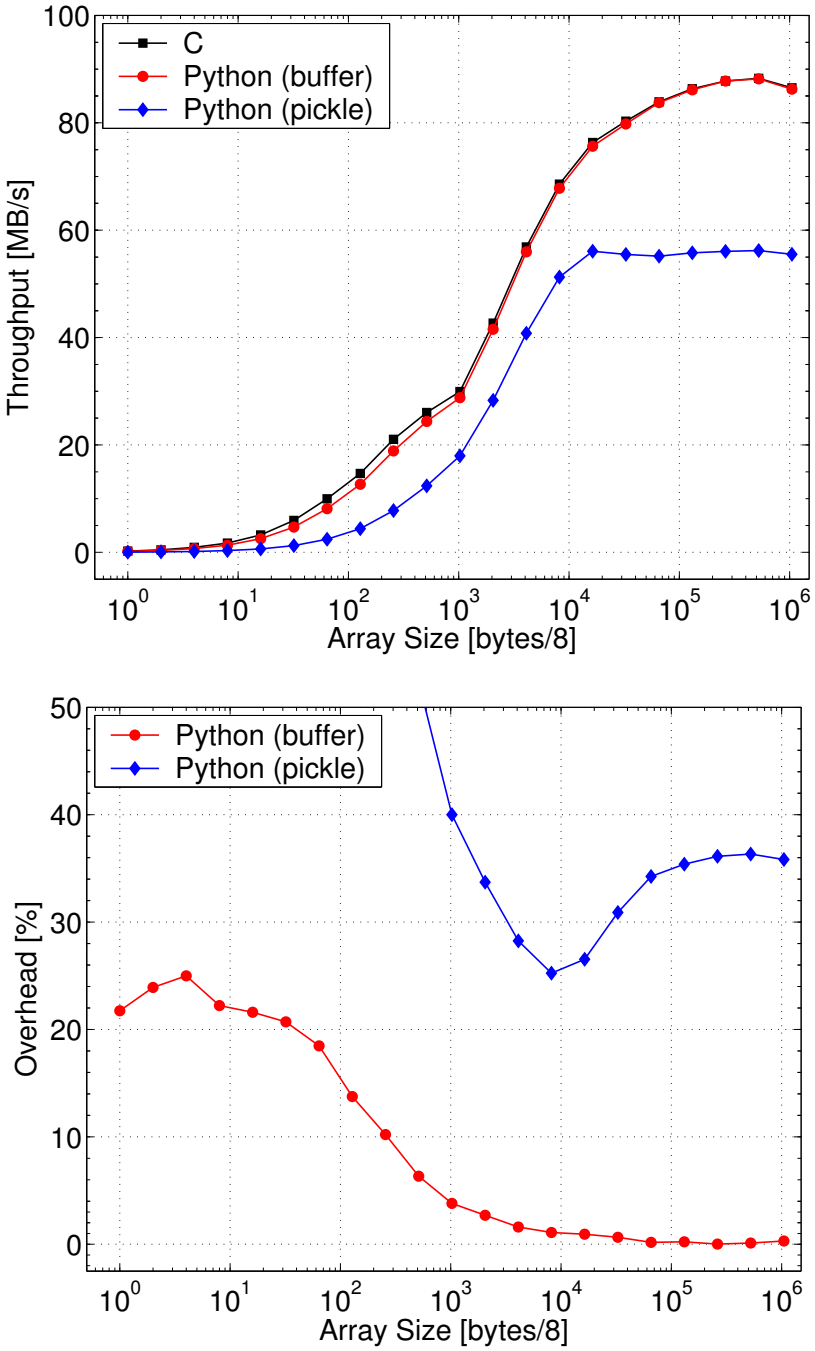

Figure 2.14: Throughput and overhead in blocking Send and Receive.

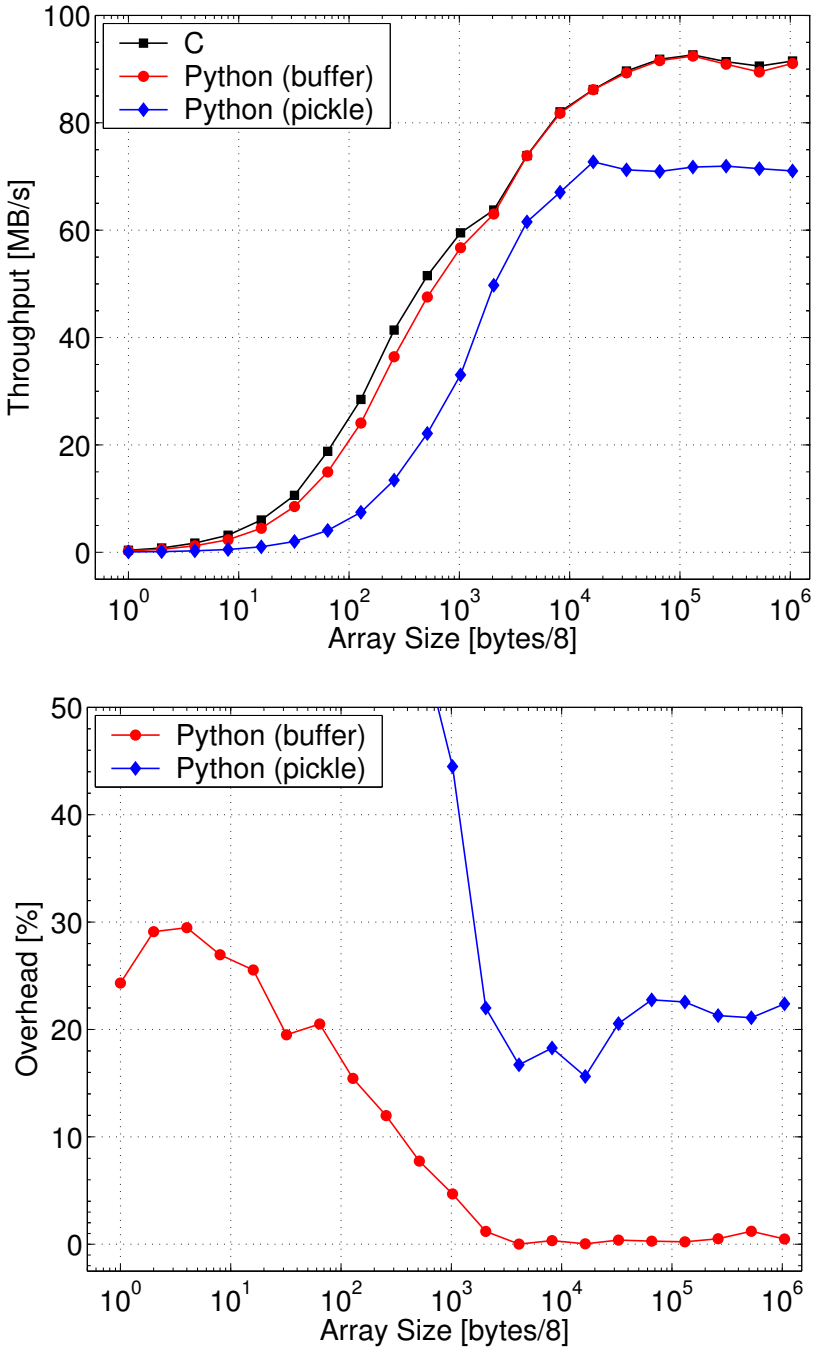

Figure 2.15: Throughput and overhead in bidirectional Send/Receive.

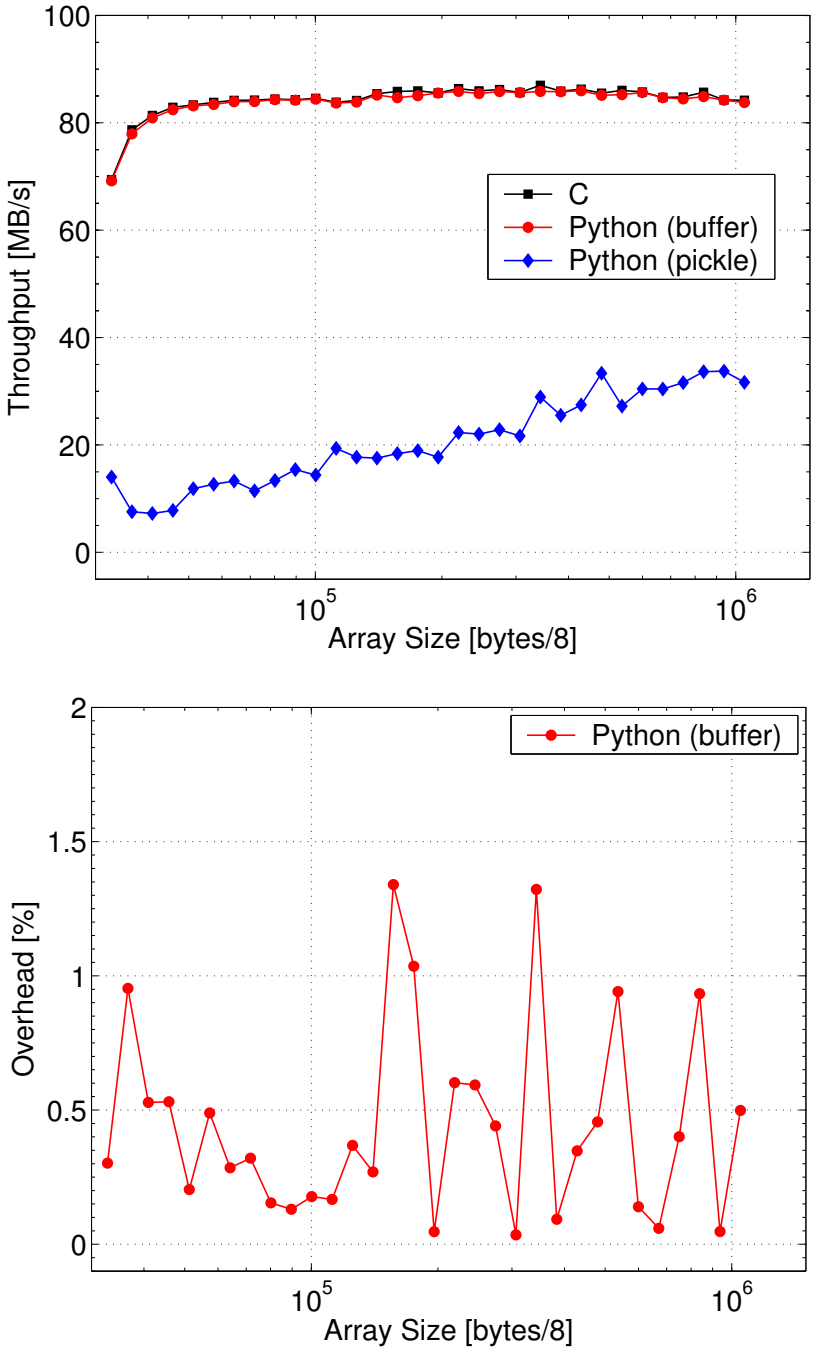

Figure 2.16: Throughput and overhead in All-To-All.

2.5.2 Comparing Wall-Clock Timings for Collective Communication Operations

Additional efficiency tests were run on the older Beowulf class cluster *Geronimo* [35]. Hardware consisted of ten computing nodes with Intel P4 2.4Ghz processors, 512KB cache size, 1024MB RAM DDR 333MHz and 3COM 3c509 (Vortex) Nic cards interconnected with an Encore ENH924-AUT+ 100Mbps Fast Ethernet switch.

Those tests consisted in wall-clock time measurements of some collective operations on ten uniprocessor nodes. Messages were again numeric arrays of double precision floating-point values. Results are shown in figures 2.17 to 2.21. For array sizes greater than 10^3 (8KB), timings in Python are between 5% (for *broadcast*) to 20% (for *all-to-all*) greater than timings in C.

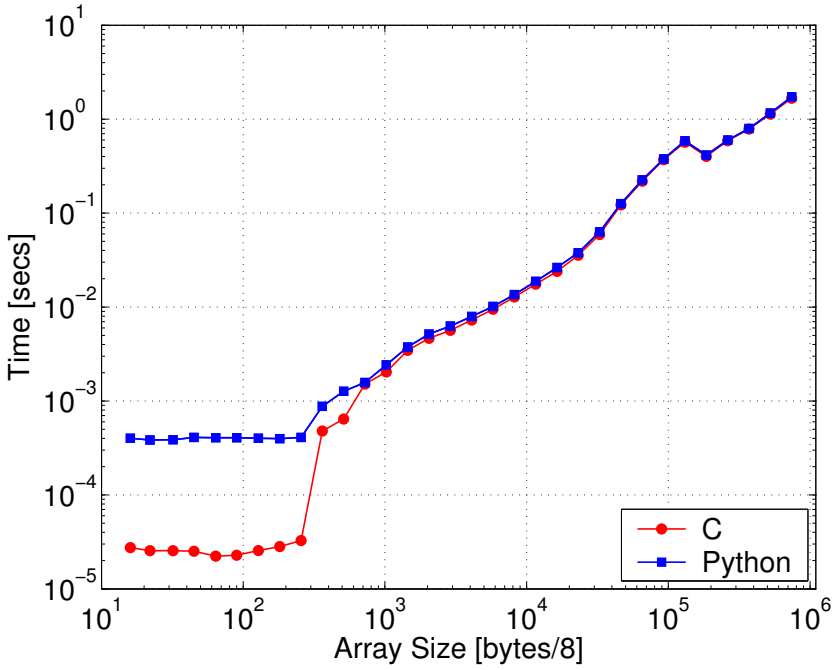

Figure 2.17: Timing in Broadcast.

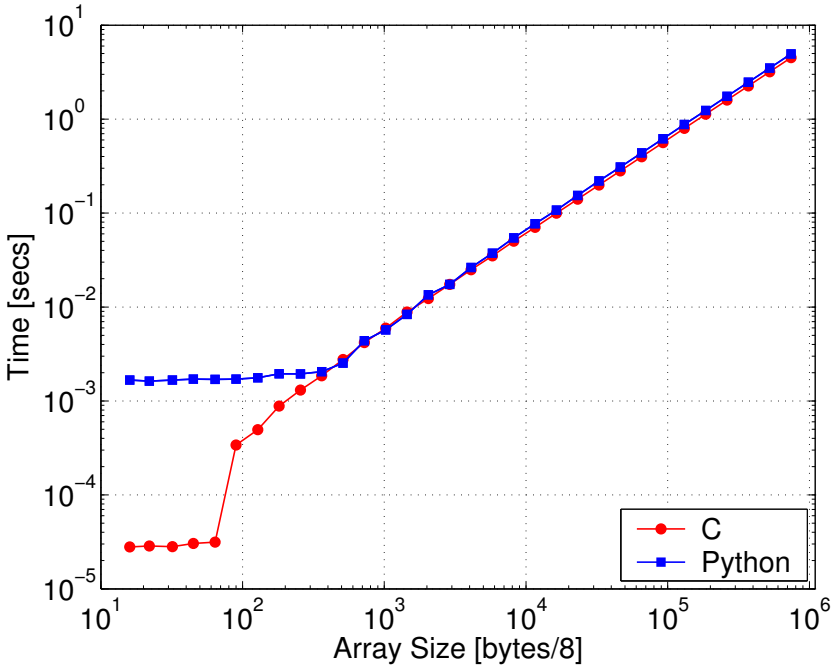

Figure 2.18: Timing in Scatter.

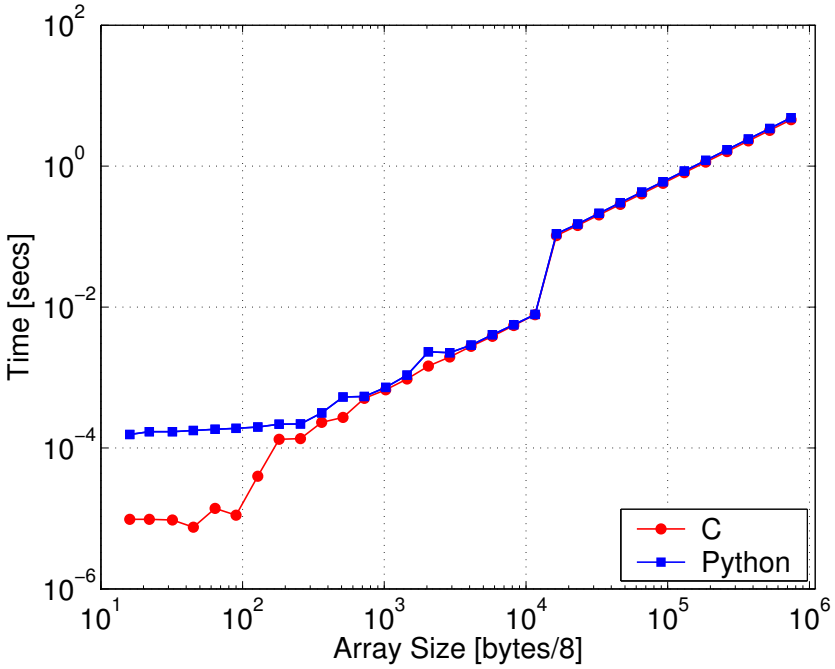

Figure 2.19: Timing in Gather.

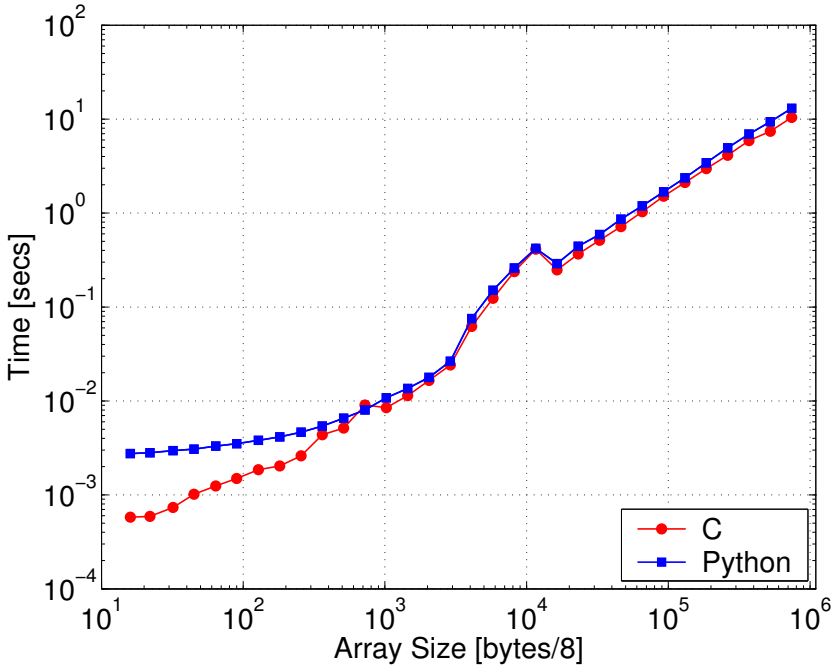

Figure 2.20: Timing in Gather to All.

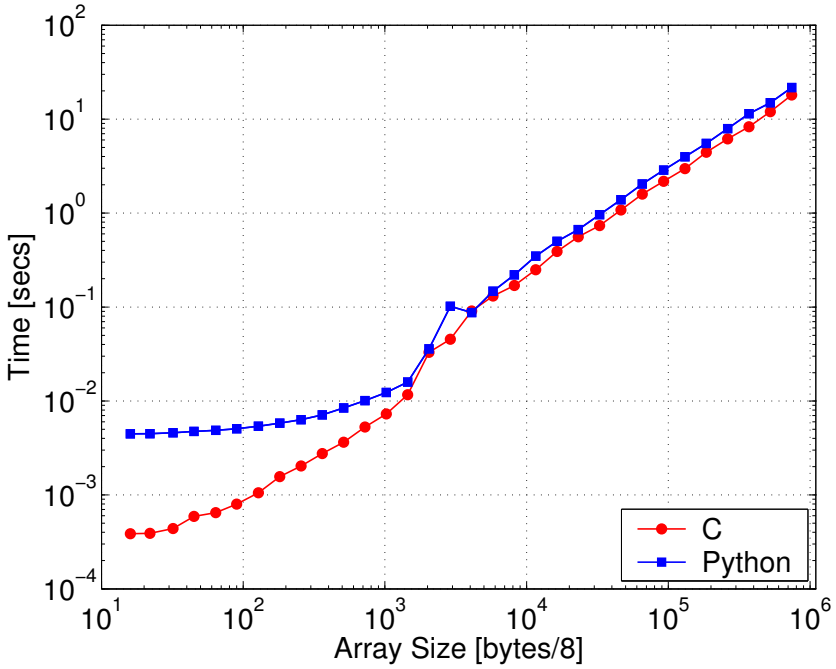

Figure 2.21: Timing in All to All Scatter/Gather.

Chapter 3

PETSc for Python

This chapter is devoted to describing PETSc for Python, an open-source, public-domain software project that provides access to the *Portable, Extensible Toolkit for Scientific Computation* (PETSc) libraries for the Python programming language.

PETSc for Python is a general-purpose and full-featured package. Its facilities allow sequential and parallel Python applications to exploit state of the art algorithms and data structures readily implemented in PETSc and targeted to large-scale numerical simulations arising in many problems of science and engineering.

Section 3.1 presents a general description about PETSc and their main components and features. Section 3.2 describes the general design and implementation of PETSc for Python through a mixed language, C-Python approach and the help of the *SWIG* interface generator.

Section 3.3 presents a general overview of the many PETSc concepts and functionalities accessible through PETSc for Python. Additionally, a series of short, self-contained example codes with their corresponding discussions is provided. These examples show how to use PETSc for Python for implementing sequential and parallel Python codes with the help of PETSc.

Finally, section 3.4 presents some efficiency tests and discusses their results. Those test are focused on determining the calling overhead introduced by the Python layer. This is done by measuring and comparing wall clock timings of

a simple sequential application implemented both in C and Python and some auxiliary Fortran code. The application is related to the numerical solution of a model linear boundary value problem using matrix-free techniques and Krylov-based iterative methods for solving the subsidiary linear systems arising from a finite differences discretization.

3.1 An Overview of PETSc

PETSc [2, 4], the *Portable Extensible Toolkit for Scientific Computation*, is a suite of algorithms and data structures for the solution of problems arising on scientific and engineering applications, specially those modeled by partial differential equations, of large-scale nature, and targeted for parallel, distributed-memory computing environments [5].

PETSc is written in C (thus making it usable from C++); a Fortran interface (very similar to the C one) is also available. The complete set of features provided by PETSc is better exploited when it is employed for implementing parallel applications. Nevertheless, PETSc perfectly supports the implementation of sequential applications.

PETSc employs the MPI standard for inter-process communication, thus it is based on the message-passing model for parallel computing. Despite this, PETSc provides many high-level functionalities that typical users needs to write very few message-passing calls on their specific codes.

Being written in C and based on MPI, PETSc is highly portable software library. PETSc-based applications can run in almost all modern parallel environment, ranging from distributed memory architectures (with standard networks as well as specialized communication hardware) to multi-processor (and multi-core) shared memory machines.

3.1.1 Main Features of PETSc

PETSc is designed with an object-oriented style. Almost all user-level objects are instances of some specific type. Those objects are managed through handles to opaque data structures which are created, accessed and destroyed by calling

appropriate library routines. Additionally, PETSc is designed to be highly modular: all of its abstractions are grouped into independent but interoperable library components. Furthermore, this modular design enables PETSc to be easily extended with several specialized parallel libraries like *HYPRE* [36], *Trilinos/ML* [37], *MUMPS* [38], *SPAI* [39], and others through an unified interface.

Vectors

The *Vec* component of PETSc provides the basic data structure for storing right-hand sides and solutions of linear and nonlinear systems of equations, representing finite-dimensional elements or vector subspaces, etc. More particularly, they are employed to store field data on nodes and cells of computational grids associated to the discretization of partial differential equations. For those kind of applications, PETSc also provides additional components like index sets and general vector scatter/gather operations. In the parallel case, those abstraction encapsulate and simplify message passing of field data.

PETSc provides two basic vector types: sequential and parallel. Sequential vectors store their entries in a contiguous array. Parallel vectors are partitioned across processes: each process owns an arbitrary length but contiguous range of the entries, which are again stored in local contiguous arrays.

Regardless of their specific type, vectors are managed through a unified interface which provide access to many common operation like dot products, computing of norms, linear combinations, point-wise operations, etc.. In the parallel case, inserting or adding values to vector entries is a simple, high-level operation: in a first step, any process can set any component of the global vector; in a second step, PETSc insures that non-local components are automatically stored in the correct location by performing any needed message passing.

Matrices

The *Mat* component of PETSc provides a large suite of routines and data structures for the efficient manipulation of matrices. PETSc provides a variety

of matrix implementations, ranging from dense to sparse, because no single matrix format is appropriate for all problems. Almost all of them are available in both sequential and parallel version.

Dense matrices store all their entries in a logically two-dimensional, column-major, contiguous array (as in the usual Fortran ordering). In the parallel case, dense matrices are row-partitioned, and each process owns an arbitrary length but contiguous range of the rows. At each process, those rows are stored in a sequential dense matrix.

Sparse matrices store only non-zero entries using many specialized formats. The default, simplest and more commonly used matrix implementation is the general sparse *AIJ* format (also known as the *Yale* sparse matrix format or *compressed sparse row* format, *CSR*). In the parallel case, sparse matrices are row-partitioned, and each process owns an arbitrary length but contiguous range of the rows. In order to efficiently implement the parallel matrix-vector product operation, the set of rows at each processor is stored in two sequential matrices: the *diagonal* part and the *off-diagonal* part. For a square global matrix, the diagonal portion is a a square sub-matrix defined by it its local rows and the corresponding columns, and the off-diagonal portion encompasses the remainder of the local matrix entries (thus being in general a rectangular sub-matrix).

Regardless of their specific type, matrices are managed through a unified interface which provide access to many common operations like matrix-matrix product, sub-matrix extraction, and matrix-vector product (a key operation for the implementation or iterative methods). In the parallel case, inserting or adding values to matrix entries is a simple, high-level operation: in a first step, any process can set any component of the global matrix; in a second step, PETSc insures that non-local components are automatically stored in the correct location by performing any needed message passing.

Linear Solvers

The combination of Krylov methods and preconditioning strategies is at the core of most modern numerical methods for the iterative solution of linear

system of equations. These problems have the general form

$$Ax = b,$$

where A denotes a non-singular linear operator, b is the right-hand-side vector, and x is the solution vector.

Iterative linear solvers and preconditioners are a key part of PETSc. All the provided functionalities are available through two independent but tightly connected, interoperable components. The *KSP* component provides implementations of many popular Krylov subspace iterative methods; the *PC* component includes a variety of preconditioners and direct (i.e., factorization-based) solution methods.

The KSP and PC abstractions provide efficient access and unified interface in the sequential and parallel cases, for both iterative and direct solution methods. In addition, users can easily customize the linear solvers, being able to set the various tolerances, algorithmic parameters, and even define custom routines for monitoring the solution process and declaring convergence.

Nonlinear Solvers

The *SNES* component of PETSc provides methods for solving systems of nonlinear equations of the form

$$\boldsymbol{F}(\boldsymbol{x}) = 0,$$

where $\boldsymbol{F} : \Re^n \rightarrow \Re^n$. Newton-like methods provide the core of the package, including both line search and trust region techniques to ensure global convergence to the solution. The general form of the n-dimensional Newton's method is

$$\boldsymbol{x}_{k+1} = \boldsymbol{x}_k - [\boldsymbol{F}'(\boldsymbol{x}_k)]^{-1}\boldsymbol{F}(\boldsymbol{x}_k), \quad k = 0, 1, \ldots,$$

where $\boldsymbol{x}_0$ is an initial approximation to the solution and $\boldsymbol{F}'(\boldsymbol{x}_k)$, the Jacobian, is non-singular at each iteration. In practice, the Newton iteration is

implemented by the following two steps:

1. (Approximately) solve $\boldsymbol{F}'(\boldsymbol{x}_k)\Delta\boldsymbol{x}_k = -\boldsymbol{F}(\boldsymbol{x}_k)$.
2. Update $\boldsymbol{x}_{k+1} = \boldsymbol{x}_k + \Delta\boldsymbol{x}_k$.

The interfaces to the various solvers are all virtually identical, even in the parallel case; the only difference in the parallel version is that each process typically forms only its local contribution to the function vector $\boldsymbol{F}$ and the Jacobian matrix $\boldsymbol{F}'$. In addition, users can easily customize the nonlinear solvers for the problem at hand. They are able to set the various tolerances, algorithmic parameters, and even define routines for monitoring and declaring convergence, thus having full control of the complete solution process.

PETSc nonlinear solvers can be used in conjunction with matrix-free techniques. In the context of solving nonlinear problem, matrix-free approaches take advantage of a combination of Newton-Krylov iterative methods. The use of Krylov-based inner linear solver within the outer Newton iteration is a crucial ingredient. Krylov methods do not require to access matrix entries. Instead, they are formulated in terms of the action of a linear operator on a given input vector. Then, the Jacobian do not have to be explicitly assembled by user-provided code on a matrix data structure, nor matrix entries have to be ever computed in any way (as is however the case if *automatic differentiation* or *colored finite differences techniques* are employed). Instead, the action of the Jacobian $\boldsymbol{F}'(\boldsymbol{x})$ on a given vector $\boldsymbol{v}$ is internally approximated with the following fist-order finite differences formula,

$$\boldsymbol{F}'(\boldsymbol{x}_k)\boldsymbol{v} \approx \frac{\boldsymbol{F}(\boldsymbol{x}_k + h\boldsymbol{v}) - \boldsymbol{F}(\boldsymbol{x}_k)}{h}$$

were h is an appropriately chosen scalar value [40, 41]. Then, the nonlinear residual function is the only required input from the application side. In order to compute an approximation to $\boldsymbol{F}'(\boldsymbol{x}_k)\boldsymbol{v}$, only one evaluation of the user-provided function $\boldsymbol{F}$ is required.

Time-steppers

The *TS* component of PETSc provides a framework for the scalable solution of ordinary differential equations arising from the discretization of time-dependent partial differential equations. In addition, it provides some pseudo-transient continuation techniques for computing steady-state solutions.

3.2 Design and Implementation

In the low-level layer, an extension module written in C provide access to all functions and predefined constants in PETSc. Additionally, this C code implements some core machinery for converting any PETSc object between its Python representation (i.e. an instance of a specific Python class) and C representation (i.e. an opaque PETSc object). All this conversion machinery is carefully designed for supporting full interoperability between the C and Python sides.

The approach described in the above paragraph is very similar to the one previously described in section 2.3. However, as the number of user-level routines available in PETSc is huge, PETSc for Python took advantage of *SWIG* (see section 1.2.4) in order to automate the generation of code connecting the C and Python sides. Furthermore, this higly interoperable C-Python interface supported on *SWIG* motivated other interesting developments; they are briefly commented in chapter 5, near the end of section 5.1.

In the high-level layer, a series of modules written in Python define all class hierarchies, methods and functions. This Python code is supported by the low-level C extension module commented above. The final user interface has some connections with the one in PETSc. However, the PETSc user interfaces are not truly object-oriented; those languages do not natively support some more advanced concepts such as classes, inheritance and polymorphism, or exception-based error checking.

The user interface provided by PETSc for Python is a truly object oriented and high-level one, being by far easier and pleasant to use than the native C and Fortran ones provided in PETSc. Readers with some basic to serious

experience on programming with PETSc will hopefully realize this fact in the following section.

3.3 Using PETSc for Python

This section presents a general overview and some examples of the many PETSc functionalities readily available in PETSc for Python. The provided examples are simple, self-contained, and implemented in a few lines of Python code. Nevertheless, they show general usage patterns of PETSc for Python for implementing linear algebra algorithms, assembling sparse matrices, and solving linear and nonlinear systems of equations within a Python programming environment.

3.3.1 Working with Vectors

PETSc for Python provides access to PETSc vectors, index sets and general vector scatter/gather operations through the `Vec`, `IS`, and `Scatter` classes respectively. By using them, the management of distributed field data is highly simplified in parallel applications.

Besides the use as containers for field data, PETSc vectors also represent algebraic entities of finite-dimensional vector spaces. For this case, the `Vec` class provides many methods for performing common linear algebra operations, like computing vector updates (`axpy()`, `aypx()`, `scale()`), inner products (`dot()`) and different kinds of norms (`norm()`).

Figure 3.1 shows a basic implementation of a Krylov-based iterative linear solver, the (unpreconditioned) conjugate gradient method.

3.3.2 Working with Matrices

PETSc for Python provides access to PETSc matrices through the `Mat` class.

New `Mat` instances are obtained by calling the `create()` method. Next, the user have to specify the row and column sizes by calling the `setSizes()` method. Finally, a call to the `setType()` method select a particular matrix implementation.

$cg(A, x, b, i_{max}, \epsilon)$:

$i \Leftarrow 0$

$r \Leftarrow b - Ax$

$d \Leftarrow r$

$\delta_0 \Leftarrow r^T r$

$\delta \Leftarrow \delta_0$

while $i < i_{max}$ and

$\delta > \delta_0 \epsilon^2$ do :

$q \Leftarrow Ad$

$\alpha \Leftarrow \dfrac{\delta}{d^T q}$

$x \Leftarrow x + \alpha d$

$r \Leftarrow r - \alpha q$

$\delta_{old} \Leftarrow \delta$

$\delta \Leftarrow r^T r$

$\beta \Leftarrow \dfrac{\delta}{\delta_{old}}$

$d \Leftarrow r + \beta d$

$i \Leftarrow i + 1$

(a) Algorithm

```
def cg(A, b, x, imax=50, eps=1e-6):
    """
    A, b, x  : matrix, rhs, solution
    imax     : maximum allowed iterations
    eps      : tolerance for convergence
    """
    # allocate work vectors
    r = b.duplicate()
    d = b.duplicate()
    q = b.duplicate()
    # initialization
    i = 0
    A.mult(x, r)
    r.aypx(-1, b)
    r.copy(d)
    delta_0 = r.dot(r)
    delta = delta_0
    # enter iteration loop
    while i < imax and \
          delta > delta_0 * eps**2:
        A.mult(d, q)
        alpha = delta / d.dot(q)
        x.axpy(+alpha, d)
        r.axpy(-alpha, q)
        delta_old = delta
        delta = r.dot(r)
        beta = delta / delta_old
        d.aypx(beta, r)
        i = i + 1
    return i, delta**0.5
```

(b) Implementation

Figure 3.1: Basic Implementation of Conjugate Gradient Method.

Matrix entries can be set (or added to existing entries) by calling the `setValues()` method. PETSc simplifies the assembling of parallel matrices. Any process can contribute to any entry. However, off-process entries are internally cached. Because of this, a final call to the `assemblyBegin()` and `assemblyEnd()` methods is required in order to communicate off-process entries to the actual owning process. Additionally, those calls prepare some internal data structures for performing efficient parallel operations like matrix-vector product. The later operation is available by calling the `mult()` method.

Figure 3.2 shows the basic steps for creating and assembling a sparse matrix in parallel. The assembled matrix is a discrete representation of the two-dimensional Laplace operator on the unit square equipped with homogeneous boundary conditions after a 5-points finite differences discretization. The grid

supporting the discretization scheme is structured and regularly spaced. Furthermore, the grid nodes have a simple contiguous block-distribution by rows on a group of processes.

```
from petsc4py import PETSc

# grid size and spacing
m, n  = 32, 32
hx = 1.0/(m-1)
hy = 1.0/(n-1)

# create sparse matrix
A = PETSc.Mat()
A.create(PETSc.COMM_WORLD)
A.setSizes([m*n, m*n])
A.setType('aij') # sparse

# precompute values for setting
# diagonal and non-diagonal entries
diagv = 2.0/hx**2 + 2.0/hy**2
offdx = -1.0/hx**2
offdy = -1.0/hy**2

# loop over owned block of rows on this
# processor and insert entry values
Istart, Iend = A.getOwnershipRange()
for I in xrange(Istart, Iend) :
    A[I,I] = diagv
    i = I//n    # map row number to
    j = I - i*n # grid coordinates
    if i> 0  : J = I-n; A[I,J] = offdx
    if i< m-1: J = I+n; A[I,J] = offdx
    if j> 0  : J = I-1; A[I,J] = offdy
    if j< n-1: J = I+1; A[I,J] = offdy

# communicate off-processor values
# and setup internal data structures
# for performing parallel operations
A.assemblyBegin()
A.assemblyEnd()
```

Figure 3.2: Assembling a Sparse Matrix in Parallel.

3.3.3 Using Linear Solvers

PETSc for Python provides access to PETSc linear solvers and preconditioners through the `KSP` and `PC` classes.

New `KSP` instances are obtained by calling the `create()` method; this call also creates automatically a companion inner preconditioner that can be retrieved with the `getPC()` method for further manipulations. The `KSP` and `PC` classes provide the `setType()` methods for the selection of a specific iterative method and preconditioning strategy. The `setTolerances()` method enable the specification of the different tolerances for declaring convergence; other algorithmic parameters can also be set. Additionally, PETSc for Python supports attaching user-defined Python function for monitoring the iterative process (by calling the `setMonitor()` method) and even define a custom convergence criteria (by calling the `setConvergenceTest()` method).

`KSP` objects have to be associated with a matrix (i.e., a `Mat` instance) representing the operator of the linear problem and a (possibly different) matrix for defining the preconditioner. This is done by calling the `setOperators()`

method. In order to actually solve a linear system of equations, the `solve()` method have to be called with appropriate vector arguments (i.e., a `Vec` instances) specifying the right hand side and the location where to build the solution.

Figure 3.3 presents and example showing the minimal required steps for creating and configuring a linear solver and its companion preconditioner in PETSc for Python. This linear solver and preconditioner combination are employed for solving a linear system involving a previously assembled parallel sparse matrix (see figure 3.2).

```
# create linear solver,
ksp = PETSc.KSP()
ksp.create(PETSc.COMM_WORLD)
# use conjugate gradients
ksp.setType('cg')
# and incomplete Cholesky
ksp.getPC().setType('icc')
```

```
# obtain sol & rhs vectors
x, b = A.getVecs()
x.set(0)
b.set(1)
# and next solve
ksp.setOperators(A)
ksp.setFromOptions()
ksp.solve(b, x)
```

Figure 3.3: Solving a Linear Problem in Parallel.

3.3.4 Using Nonlinear Solvers

PETSc for Python provides access to PETSc nonlinear solvers through the `SNES` class.

New `SNES` instances are obtained by calling the `create()` method. This call also creates automatically a companion inner linear solver (i.e., a `KSP` instance) that can be retrieved with the `getKSP()` method for further manipulations. The `setTolerances()` method enable the specification of the different tolerances for declaring convergence; other algorithmic parameters can also be set. Additionally, PETSc for Python supports attaching user-defined Python functions for monitoring the iterative process (by calling the `setMonitor()` method) and even define a custom convergence criteria (by calling the `setConvergenceTest()` method).

`SNES` objects have to be associated with two user-defined Python functions in charge of evaluating the nonlinear residual vector and the Jacobian matrix at each nonlinear iteration step. Those user routines can be set with the methods `setFunction()` and `setJacobian()`.

In order to actually solve a nonlinear system of equations, the `solve()` method have to be called with appropriate vector arguments (i.e., a `Vec` instances) specifying an optional right hand side (usually not provided as it is the zero vector) and the location where to build the solution (which additionally can specify an initial guess for starting the nonlinear loop).

Consider the following boundary value problem in two dimensions:

$$\begin{aligned} -\Delta U(x) &= \alpha \exp[U(x)], \quad && x \in \Omega, \\ U(x) &= 0, && x \in \partial\Omega; \end{aligned}$$

where Ω is the unit square $(0,1)^2$ and $\partial\Omega$ is the boundary, Δ is the two-dimensional Laplace operator, and U is a scalar field defined on Ω, and α is a constant. The equation is nonlinear and usually called the Bratu problem. As α approaches the limit $\alpha_{FK} \approx 6.80812$ (the Frank-Kamenetskii parameter) the non-linearity of the problem increases; beyond that limit there is no solution.

For the sake of simplicity, assume that finite differences with the standard 5-point stencil are employed for performing a spatial discretization on structured, regularly spaced grid. As the result of the discretization process, a discrete system of nonlinear equation is obtained.

Figure 3.4 presents two possible (sequential) implementations of the nonlinear residual function $F(x) = -\Delta U(x) - \alpha \exp[U(x)]$ for the Bratu problem. The Python implementation in figure 3.4a takes advantage of multi-dimensional array processing facilities of *NumPy* arrays. The Fortran 90 implementation in figure 3.4b takes advantage of multi-dimensional Fortran 90 arrays and array pointers; it can be easily made available to Python codes by using *F2Py* interface generator. Both implementations are almost identical regarding syntax and semantics. Of course, the Fortran one is expected to execute faster.

In figure 3.5, the Python/*NumPy* implementation of the nonlinear residual function in figure 3.4a is employed for solving the Bratu problem by using a PETSc nonlinear solver through PETSc for Python. The inner Krylov linear solver is configured to use conjugate gradient method. Additionally, the nonlinear solver is configured to use a matrix-free method.

```
# file: bratu2dnpy.py

def bratu2d(alpha, x, f):
    # get 'exp' from numpy
    from numpy import exp
    # setup 5-points stencil
    u  = x[1:-1, 1:-1] # center
    uN = x[1:-1,  :-2] # north
    uS = x[1:-1, 2:  ] # south
    uW = x[ :-2, 1:-1] # west
    uE = x[2:,   1:-1] # east
    # compute nonlinear function
    nx, ny = x.shape
    hx = 1.0/(nx-1) # x grid spacing
    hy = 1.0/(ny-1) # y grid spacing
    f[:,:] = x
    f[1:-1, 1:-1] = \
         (2*u - uE - uW) * (hy/hx) \
       + (2*u - uN - uS) * (hx/hy) \
       - alpha * exp(u)  * (hx*hy)
```

(a) Python/*NumPy* version

```
! file: bratu2dlib.f90
! to build a Python module, use this:
! $$ f2py -m bratu2dlib -c bratu2dlib.f90

subroutine bratu2d (m, n, alpha, x, f)
  !f2py intent(hide) :: m = shape(x,0)
  !f2py intent(hide) :: n = shape(x,1)
  integer                          :: m, n
  real(kind=8)                     :: alpha
  real(kind=8), intent(in), target :: x(m,n)
  real(kind=8), intent(inout)      :: f(m,n)
  real(kind=8) :: hx, hy
  real(kind=8), pointer, &
       dimension(:,:) :: u, uN, uS, uE, uW
  ! setup 5-points stencil
  u  => x(2:m-1, 2:n-1) ! center
  uN => x(2:m-1, 1:n-2) ! north
  uS => x(2:m-1, 3:n  ) ! south
  uW => x(1:m-2, 2:n-1) ! west
  uE => x(3:m,   2:n-1) ! east
  ! compute nonlinear function
  hx = 1.0/(m-1) ! x grid spacing
  hy = 1.0/(n-1) ! y grid spacing
  f(:,:) = x
  f(2:m-1, 2:n-1) =  &
         (2*u - uE - uW) * (hy/hx) &
       + (2*u - uN - uS) * (hx/hy) &
       - alpha * exp(u)  * (hx*hy)
end subroutine bratu2d
```

(b) Fortran 90 version

Figure 3.4: Nonlinear Residual Function for the Bratu Problem.

```
from petsc4py import PETSc
from bratu2dnpy import bratu2d

# this user class is an application
# context for the nonlinear problem
# at hand; it contains some parametes
# and knows how to compute residuals

class Bratu2D:

    def __init__(self, nx, ny, alpha):
        self.nx = nx # x grid size
        self.ny = ny # y grid size
        self.alpha = alpha
self.compute = bratu2d


    def evalFunction(self, snes, X, F):
        nx, ny = self.nx, self.ny
        alpha = self.alpha
        x = X[...].reshape(nx, ny)
        f = F[...].reshape(nx, ny)
        self.compute(alpha, x, f)
```

```
# create application context
# and nonlinear solver
nx, ny = 32, 32 # grid sizes
alpha  = 6.8
appd = Bratu2D(nx, ny, alpha)
snes = PETSc.SNES().create()

# register the function in charge of
# computing the nonlinear residual
f = PETSc.Vec().createSeq(nx*ny)
snes.setFunction(appd.evalFunction, f)

# configure the nonlinear solver
# to use a matrix-free Jacobian
snes.setUseMF(True)
snes.getKSP().setType('cg')
snes.setFromOptions()

# solve the nonlinear problem
b, x = None, f.duplicate()
x.set(0) # zero inital guess
snes.solve(b, x)
```

Figure 3.5: Solving a Nonlinear Problem with Matrix-Free Jacobians.

3.4 Efficiency Tests

In the context of scientific computing, Python is commonly used as glue language for interconnecting different pieces of codes written in compiled languages like C, C++ and Fortran. By using this approach, complex scientific applications can take advantage of the best features of both worlds: the convenient, high-level programming environment of Python and the efficiency of compiled languages for numerically intensive computations.

This section presents some efficiency tests targeted to measure the overhead of accessing PETSc functionalities through PETSc for Python. The overhead is determined by comparing the wall-clock running time of equivalent driving codes implemented in Python and C. Both codes employ PETSc iterative linear solvers and an auxiliary Fortran routine in charge of performing application-specific computations. The actual application deals with the numerical solution of a model linear partial differential equation using Krylov-based iterative linear solvers in combination with matrix-free techniques.

3.4.1 The Poisson Problem

Consider the following Poisson problem in three dimensions equipped with homogeneous boundary conditions:

$$\begin{aligned} -\Delta\phi &= 1 \text{ on } \Omega, \\ \phi &= 0 \text{ at } \Gamma; \end{aligned}$$

where Ω is the unit box $(0,1)^3$ and Γ is the entire box boundary, Δ is the three-dimensional Laplace operator, and ϕ is a scalar field defined on Ω.

From the many discretization methods suitable for the above problem, finite differences is the chosen one; this method can be easily and efficiency implemented in Fortran 90 with a few lines of code. Thus, the spatial discretization is performed with finite differences using the standard 7-points stencil on a structured, regularly spaced grid. For the sake of simplicity, the discrete grid is assumed to have the same number of nodes on each of its three directions. For a given discrete grid having $n+2$ points in each direction, a system of lin-

ear equations with n^3 equations and n^3 unknowns is obtained. The associated discrete linear operator is symmetric and positive definite.

3.4.2 A Matrix-Free Approach for the Linear Problem

The system of linear equations arising from the spatial discretization can be approximately solved by using Krylov-based iterative methods. Those methods are suitable for employing *matrix-free* representations of linear operators. In matrix-free techniques, the entries of the linear system matrix are not explicitly stored. Instead, the linear operator is implicitly defined by its action on a given input vector.

Figure 3.6 shows the complete implementation of a matrix-free linear operator for the problem at hand. In figure 3.6b, the auxiliary Fortran code implements a routine in charge of computing the action of the (negative) discrete Laplacian. This implementation takes advantage of multi-dimensional array processing; a careful look reveals that an auxiliary input array is being employed in order to simplify the handling of boundary conditions. This routine is easily made available to Python by using *F2Py*. In figure 3.6a, a Python class implements some selected methods of the generic interface for user-defined linear operators. The `mult()` method receives the input and output vectors and calls the previously discussed Fortran routine in order to actually compute the action of the discrete Laplace operator. Other two additional methods are also implemented: `multTranspose()` and `getDiagonal()`.

Figure 3.7 shows how the previous codes are combined in order to actually solve the linear system of equations. A *shell* PETSc matrix is created with appropriate row and column sizes. This matrix is associated with an instance of the user-defined matrix class previously implemented as shown in figure 3.6. From the matrix object, appropriately sized vectors for storing the solution and right hand side are obtained; all right hand side vector entries are set to one. Next, a PETSc linear solver is created and configured to use conjugate gradients with no preconditioner. Finally, the linear system of equations is solved and the solution vector is scaled in order to account for the grid spacing.

For the sake of completeness, figures 3.8 and 3.9 show a complete C im-

```
# file: del2mat.py

from numpy import zeros
from del2lib import del2apply

class Del2Mat:

    def __init__(self, n):
        self.N = (n, n, n)
        self.F = zeros([n+2]*3, order='f')

    def mult(self, x, y):
        "y <- A * x"
        N, F = self.N, self.F
        # get 3D arrays from vectos
        xx = x[...].reshape(N, order='f')
        yy = y[...].reshape(N, order='f')
        # call Fortran subroutine
        del2apply(F, xx, yy)

    def multTranspose(self, x, y):
        "y <- A' * x"
        self.mult(x, y)

    def getDiagonal(self, D):
        "D[i] <- A[i,i]"
        D[...] = 6.0
```

(a) Python class defining a *shell* matrix

```
! file: del2lib.f90

! to build a Python module, use this:
! $$ f2py -m del2lib -c del2lib.f90

subroutine del2apply (n, F, x, y)

  !f2py intent(hide) :: n=shape(F,0)-2
  integer      :: n
  real(kind=8) :: F(0:n+1,0:n+1,0:n+1)
  real(kind=8) :: x(n,n,n)
  real(kind=8) :: y(n,n,n)

  F(1:n,1:n,1:n) = x

  y(:,:,:) = 6.0 * F(1:n,1:n,1:n) &
           - F(0:n-1,1:n,1:n)     &
           - F(2:n+1,1:n,1:n)     &
           - F(1:n,0:n-1,1:n)     &
           - F(1:n,2:n+1,1:n)     &
           - F(1:n,1:n,0:n-1)     &
           - F(1:n,1:n,2:n+1)

end subroutine del2apply
```

(b) Finite differences in Fortran 90

Figure 3.6: Defining a Matrix-Free Operator for the Poisson Problem.

```
from petsc4py import PETSc
from del2mat import Del2Mat

# number of nodes in each direction
# excluding those at the boundary
n = 32
h = 1.0/(n+1) # grid spacing

# setup linear system matrix
A = PETSc.Mat().create()
A.setSizes([n**3, n**3])
A.setType('shell')
shell = Del2Mat(n) # shell context
A.setShellContext(shell)

# setup linear system vectors
x, b = A.getVecs()
x.set(0.0)
b.set(1.0)

# setup Krylov solver
ksp = PETSc.KSP().create()
pc = ksp.getPC()
ksp.setType('cg')
pc.setType('none')
ksp.setFromOptions()

# iteratively solve linear
# system of equations A*x=b
ksp.setOperators(A)
ksp.solve(b, x)

# scale solution vector to
# account for grid spacing
x.scale(h**2)
```

Figure 3.7: Solving a Matrix-Free Linear Problem with PETSc for Python.

plementation equivalent to the Python one previously discussed and shown in figures 3.6a and 3.7. This C code reuses the Fortran subroutine implementing the finite difference scheme shown in figure 3.6b.

3.4.3 Some Selected Krylov-Based Iterative Methods

Conjugate gradient iterations are the natural choice for iteratively solving a system of linear equations with symmetric and positive definite operators. However, the solution of linear problem at hand can also be found with other Krylov-based linear solvers tailored to more general problems. For the testing purposes of this section, four different solvers readily implemented in PETSc and available through PETSc for Python are employed.

The following list summarizes some aspects of the selected Krylov-based iterative methods regarding to their applicability, storage requirements (work vectors) for the unpreconditioned versions and involved computational kernels (vector inner products, vector updates, and matrix-vector products). For further details, see [42] and references therein.

- **Conjugate Gradient Method** (*CG*): this method is suitable for symmetric and positive definite linear problems. *CG* requires very few memory resources: it can be implemented with just two work vectors. At each iteration, *CG* requires a small, fixed amount of computation (two inner products and three vector updates) and only one matrix-vector product.
- **Minimal Residual Method** (*MINRES*): this method is suitable for symmetric indefinite linear problems. *MINRES* requires eight work vectors and the computation of more vector primitives than *CG*. However, *MINRES* can be employed in any symmetric problem, not just the positive definite ones. At each iteration, *MINRES* requires a fixed amount computation and only one matrix-vector product.
- **BiConjugate Gradient Stabilized** (*BiCGStab*): this method is suitable for general linear problems. *BiCGStab* requires five additional work vectors. At each iteration, *BiCGStab* requires a moderated and fixed amount computation (four inner products and six vector updates) and two matrix-vector products.

```
/* file: del2mat.h */

#ifndef DEL2MAT_H
#define DEL2MAT_H

#include <petsc.h>
#include <petscvec.h>
#include <petscmat.h>

/* external Fortran subroutine */
#define Del2Apply del2apply_
extern void Del2Apply(int*,double*,double*,double*);

/* user data structure and routines
 * defining the matrix-free operator */

typedef struct {
  PetscInt    N;
  PetscScalar *F;
} Del2Mat;

#undef  __FUNCT__
#define __FUNCT__ "Del2Mat_mult"
/* y <- A * x */
PetscErrorCode Del2Mat_mult(Mat A, Vec x, Vec y)
{
  Del2Mat *ctx;
  PetscScalar *xx,*yy;
  PetscErrorCode ierr;
  PetscFunctionBegin;
  ierr = MatShellGetContext(A,(void**)&ctx);CHKERRQ(ierr);
  /* get raw vector arrays */
  ierr = VecGetArray(x,&xx);CHKERRQ(ierr);
  ierr = VecGetArray(y,&yy);CHKERRQ(ierr);
  /* call external Fortran subroutine */
  Del2Apply(&ctx->N,ctx->F,xx,yy);
  /* restore raw vector arrays */
  ierr = VecRestoreArray(x,&xx);CHKERRQ(ierr);
  ierr = VecRestoreArray(y,&yy);CHKERRQ(ierr);
  PetscFunctionReturn(0);
}
#undef  __FUNCT__
#define __FUNCT__ "Del2Mat_diag"
/*D_i <- A_ii */
PetscErrorCode Del2Mat_diag(Mat A, Vec D)
{
  PetscErrorCode ierr;
  PetscFunctionBegin;
  ierr = VecSet(D,6.0);CHKERRQ(ierr);
  PetscFunctionReturn(0);
}

#endif
```

Figure 3.8: Defining a Matrix-Free Operator, C implementation.

```
#include "del2mat.h"
#include <petscksp.h>

#define DEL2MAT_MULT   ((void(*)(void))Del2Mat_mult)
#define DEL2MAT_DIAG   ((void(*)(void))Del2Mat_diag)

int main(int argc,char **argv)
{
  PetscInt n;
  PetscScalar h;
  Del2Mat shell;
  Mat A;
  Vec x,b;
  KSP ksp;
  PC  pc;
  /* PETSc initialization  */
  PetscInitialize(&argc, &argv, PETSC_NULL, PETSC_NULL);
  /* number of nodes in each direction
   * excluding those at the boundary */
  n = 32;
  h = 1.0/(n+1); /* grid spacing */
  /* setup linear system (shell) matrix */
  MatCreate(PETSC_COMM_SELF, &A);
  MatSetSizes(A, n*n*n, n*n*n, n*n*n, n*n*n);
  MatSetType(A, MATSHELL);
  shell.N = n;
  PetscMalloc((n+2)*(n+2)*(n+2)*sizeof(PetscScalar),&shell.F);
  PetscMemzero(shell.F, (n+2)*(n+2)*(n+2)*sizeof(PetscScalar));
  MatShellSetContext(A, (void**)&shell);
  MatShellSetOperation(A, MATOP_MULT,           DEL2MAT_MULT);
  MatShellSetOperation(A, MATOP_MULT_TRANSPOSE, DEL2MAT_MULT);
  MatShellSetOperation(A, MATOP_GET_DIAGONAL,   DEL2MAT_DIAG);
  /* setup linear system vectors */
  MatGetVecs(A, &x, &b);
  VecSet(x, 0);
  VecSet(b, 1);
  /* setup Krylov linear solver */
  KSPCreate(PETSC_COMM_SELF, &ksp);
  KSPGetPC(ksp, &pc);
  KSPSetType(ksp, KSPCG); /* use conjugate gradients */
  PCSetType(pc, PCNONE);  /* with no preconditioning */
  KSPSetFromOptions(ksp);
  /* iteratively solve linear system of equations A*x=b */
  KSPSetOperators(ksp,A,A,SAME_NONZERO_PATTERN);
  KSPSolve(ksp, b, x);
  /* scale solution vector to account for grid spacing */
  VecScale(x, h*h);
  /* free memory and destroy objects */
  PetscFree(shell.F);
  MatDestroy(A);
  VecDestroy(x);
  VecDestroy(b);
  KSPDestroy(ksp);
  /* finalize PETSc */
  PetscFinalize();
  return 0;
}
```

Figure 3.9: Solving a Matrix-Free Linear Problem, C implementation.

- **Generalized Minimal Residual Method** (*GMRES*): this method is suitable for general linear problems. While iterating, *GMRES* construct a orthonormal basis for the Krylov subspace by inserting new vectors obtained through some orthogonalization procedure. Therefore, *GMRES* requires an additional work vector and an increasing amount of computation ($i+1$ inner products and $i+1$ vector updates, being i the iteration number) of at each new iteration. Practical implementations limit the size of the Krylov basis by *restarting* the iterative process; this variant is usually denoted as $GMRES(m)$, where m is the maximum size of the Krylov basis. At each iteration, *GMRES* requires only one matrix-vector product.

3.4.4 Measuring Overhead

Tests were run sequentially on one computing node of the cluster *Aquiles* [34]. The software and hardware components were the ones previously described in section 2.5. Additionally, *PETSc 2.3.3-p6* was employed.

Results are shown in figures 3.11, 3.13, 3.15, and 3.17. The overhead is determined as $(T_{Py}/T_C) - 1$, where T_{Py} and T_C are the measured wall clock times spent by the Python implementation (see figures 3.6 and 3.7) and the C implementation (see figures 3.8 and 3.9) respectively in solving the problem at hand for different levels of discretization. Additionally, figures 3.11, 3.13, 3.15, and 3.17 show the convergence histories of the methods for some selected number of unknowns.

The general trend is the expected one: as the number of unknowns grows, the overhead of PETSc for Python diminishes. Figure 3.10 shows together the results for the *CG* and *GMRES* cases. *CG* method exhibits greater overhead for a given problem size. Indeed, of the four methods *CG* and *BiCGStab* are the ones with the lowest amount of vector-vector operations versus matrix-vector operations. Therefore, the overhead of applying the matrix-vector product from the Python layers is more significant. On the other way, *GMRES* exhibits the lowest overhead, as it is the method requiring the highest amount of inner vector-vector operations.

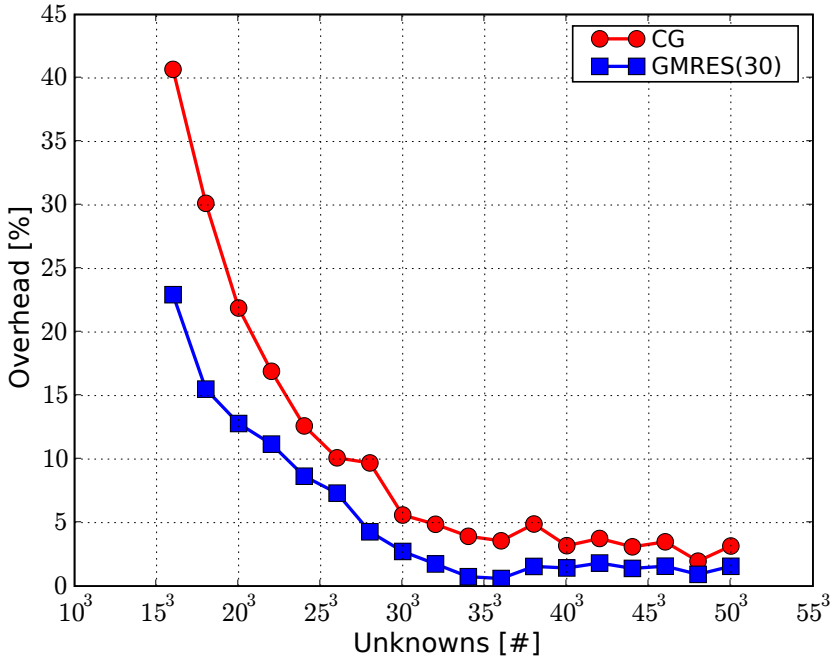

Figure 3.10: Comparing Overhead Results for *CG* and *GMRES*(30).

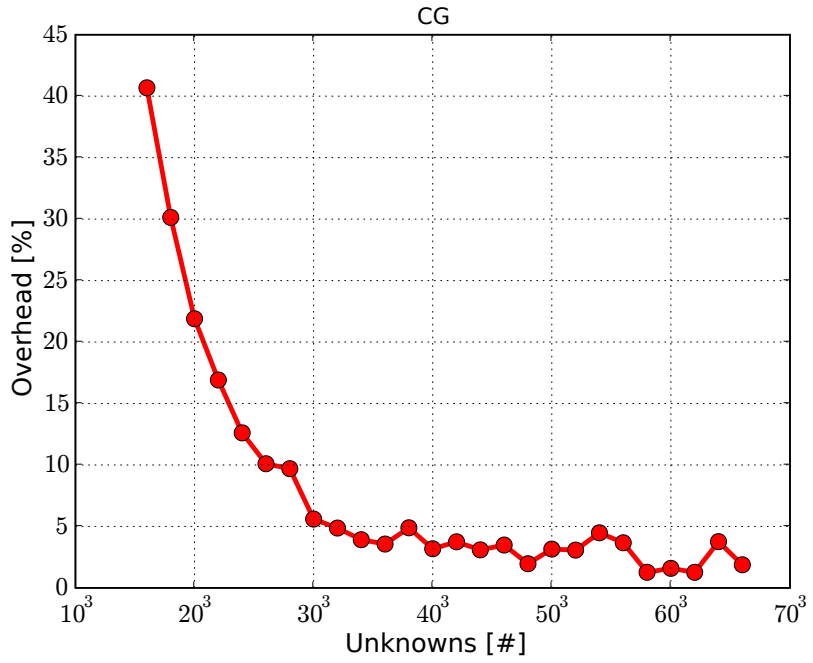

Figure 3.11: PETSc for Python Overhead using *CG*.

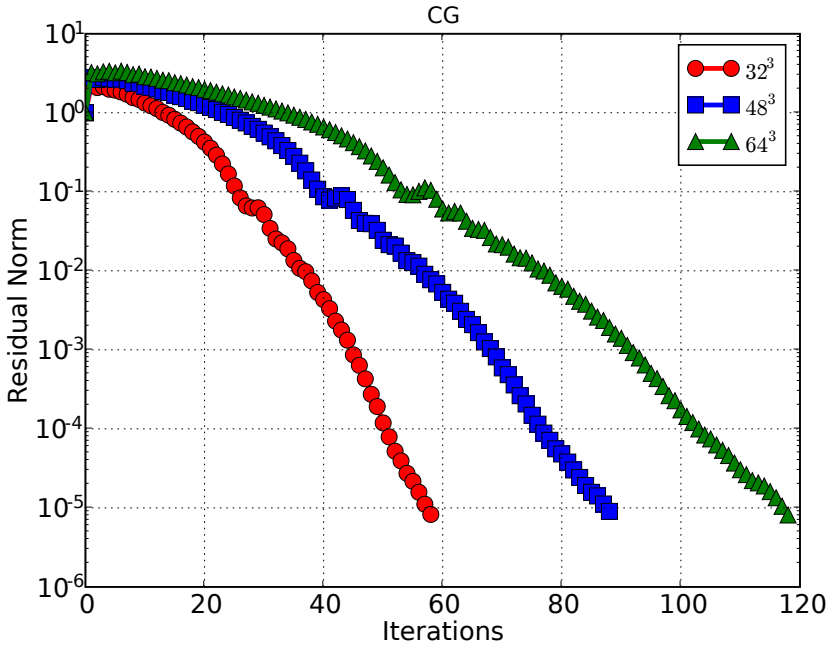

Figure 3.12: Residual History using *CG*.

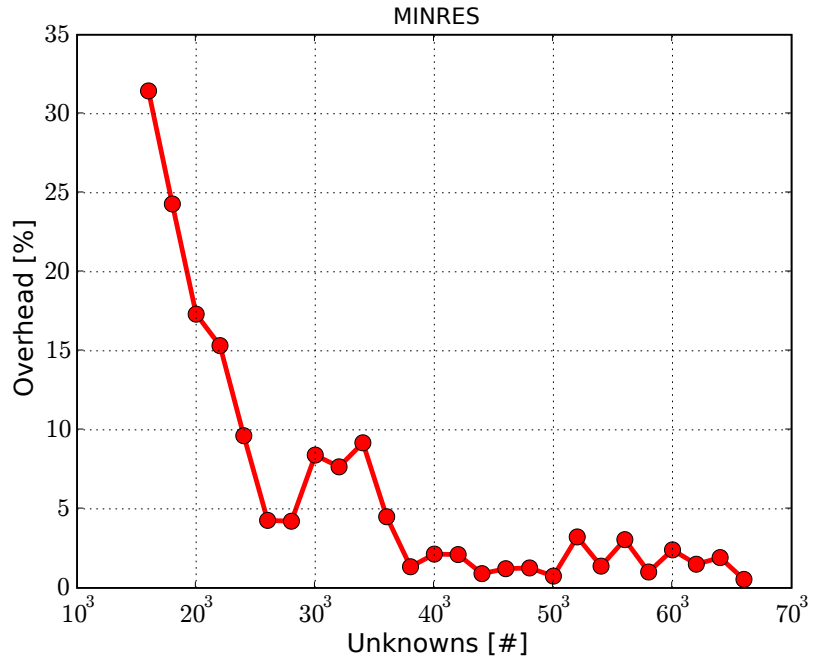

Figure 3.13: PETSc for Python Overhead using *MINRES*.

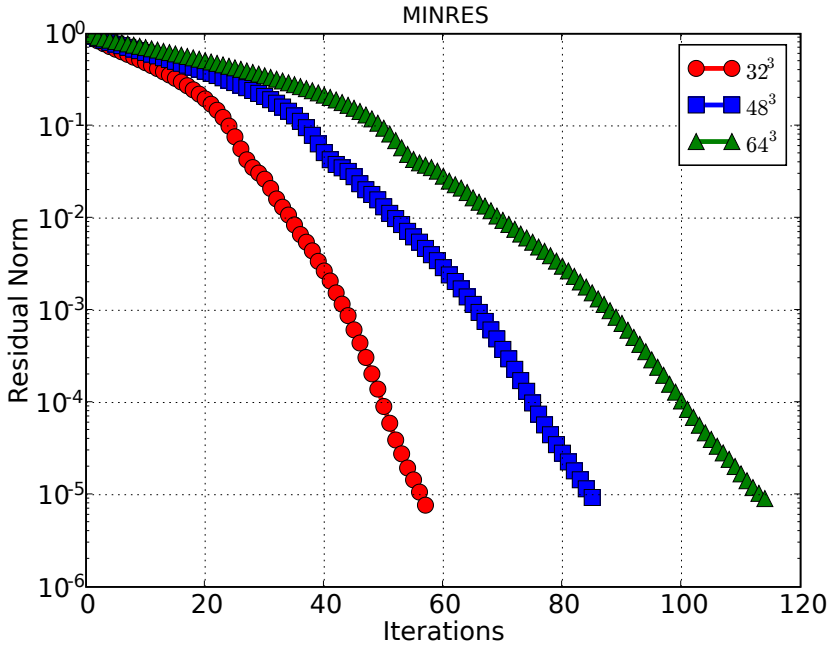

Figure 3.14: Residual History using *MINRES*.

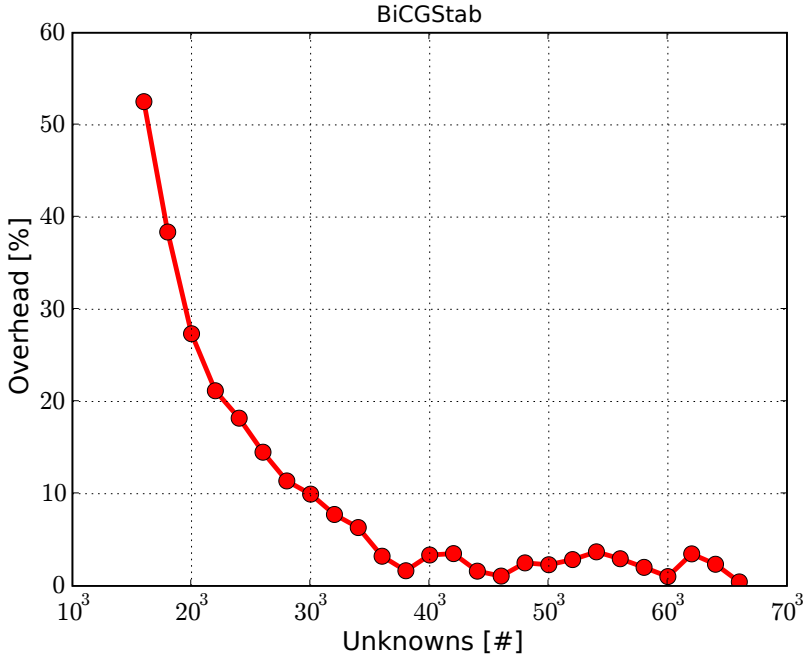

Figure 3.15: PETSc for Python Overhead using *BiCGStab*.

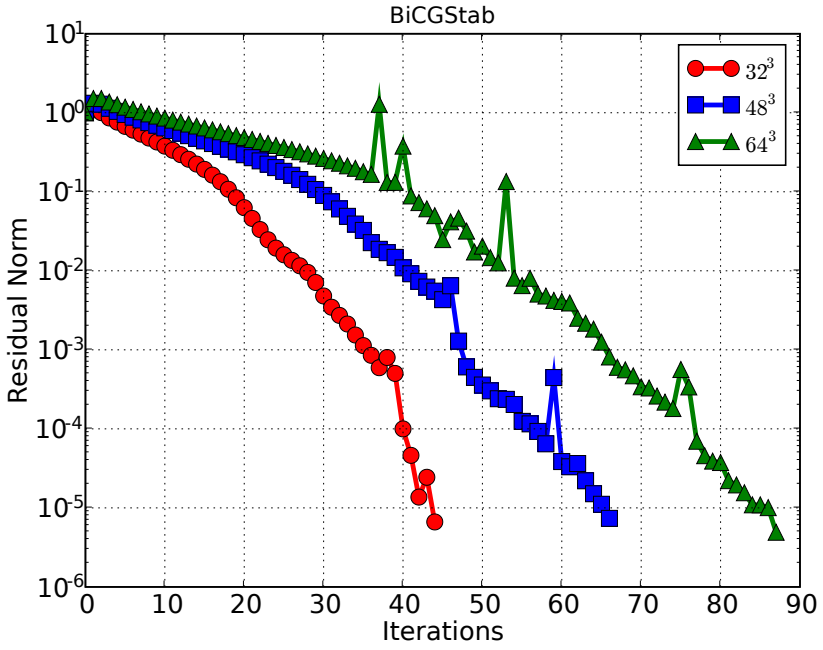

Figure 3.16: Residual History using *BiCGStab*.

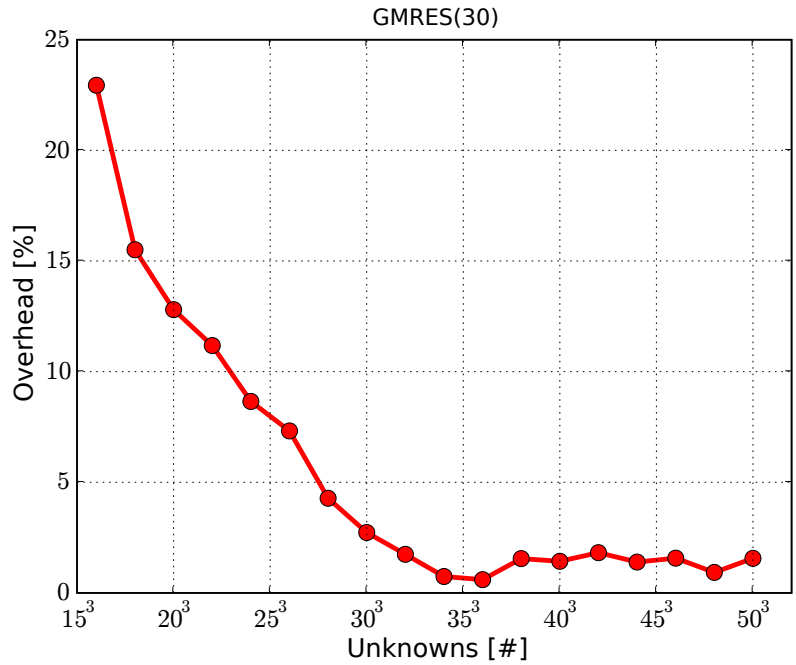

Figure 3.17: PETSc for Python Overhead using $GMRES(30)$.

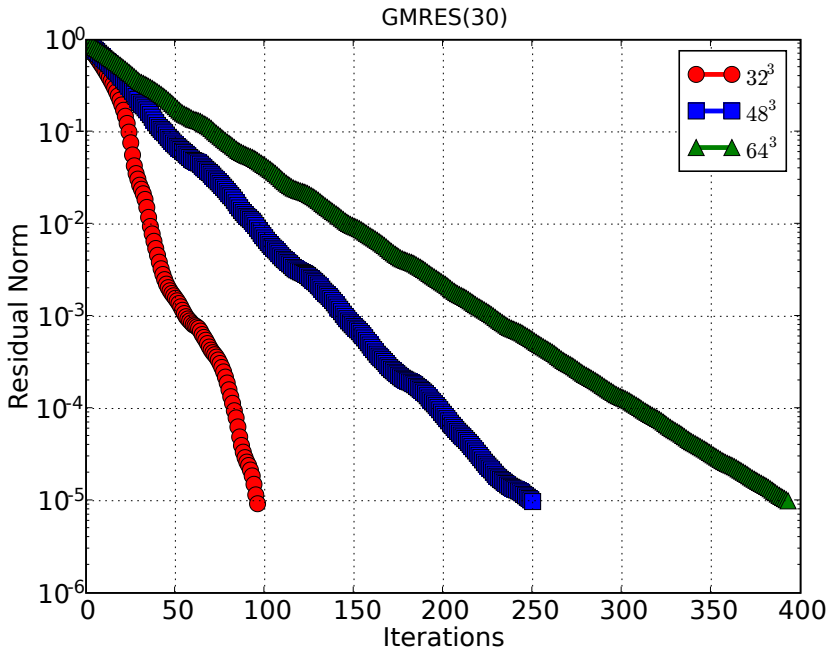

Figure 3.18: Residual History using $GMRES(30)$.

Chapter 4

Electrokinetic Flow in Microfluidic Chips

This chapter discusses the theoretical modeling and numerical simulations of electrokinetic and transport phenomena in microfluidic chips, considering effects in three dimensions and whole geometries. The modeling grounds on conservation equations of mass, momentum and electric charge in the framework of continuum mechanics. An example of interest in electrophoresis chips is considered as study case.

All numerical simulations presented in this chapter are performed with *PETSc-FEM* [12, 43] within the Python programming environment described in previous chapters. PETSc-FEM is a parallel multi-physics code primarily targeted to 2D and 3D finite elements computations on general unstructured grids. PETSc-FEM is based on MPI and PETSc, it is being developed since 1999 at the *International Center for Numerical Methods in Engineering* (CIMEC), Argentina. PETSc-FEM provides a core library in charge of managing parallel data distribution and assembly of residual vectors and Jacobian matrices, as well as facilities for general tensor algebra computations at the level of problem-specific finite element routines. Additionally, PETSc-FEM provides a suite of specialized application programs built on top of the core library but targeted to a variety or problems (e.g., compressible/incompressible Navier–Stokes and compressible Euler equations, general

advective-diffusive systems, weak/strong fluid-structure interaction). In particular, fluid flow computations presented in this chapter are carried out within the Navier–Stokes module available in *PETSc-FEM*. This module provides the required capabilities for simulating incompressible fluid flow through a monolithic *SUPG/PSPG* [44, 45] stabilized formulation for linear finite elements.

4.1 Background

Microfluidic chips or *micro Total Analysis Systems* (μ–TAS) perform the functions of large analytical devices in small units [46]. They are used in a variety of chemical, biological and medical applications. The benefits of μ–TAS are a reduction of consumption of samples and reagents, shorter analysis times, greater sensitivity, portability and disposability. There has been a huge interest in these devices in the past decade that led to a commercial range of products by Caliper, Agilent, Shimadzu and Hitachi [47].

Most microfluidic systems have been successfully fabricated in glass or oxidized silicon [48]. Microscopic channels are defined in these substrates using *photolithography* and *micromachining*, whose materials and fabrication methods were adopted from the microelectronics industry. However, for the purposes of rapid prototyping and testing of new concepts, the fabrication processes are slow and expensive.

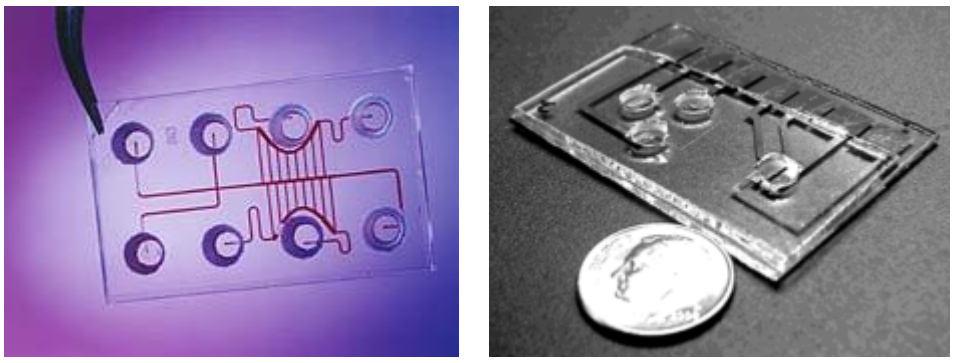

Figure 4.1: Microfluidic Chips.

Numerical simulations of on-chip processes can serve to reduce the time from concept to chip [49]. Some of the first numerical simulations of flow and species transport for microfluidic chips were based on electrokinetic focusing and sample dispensing techniques. Patankar and Hu [50] employed an algorithm based on a finite differences discretization of the governing equations on a structured grid to simulate those techniques. Bianchi et al. [51] performed 2D finite element simulations artificially increasing the electric double layer thickness. 3D finite volume simulations have been also performed [52, 53]. Erickson [54] investigated electroosmotic flow in heterogeneous surfaces with a 3D finite element model on a simultaneous solution to the Nernst–Planck, Poisson and Navier–Stokes equations.

Microfluidic chips developed for *capillary electrophoresis* integrates a network of microchannels, reservoirs and electrodes, as the transport of fluids is driven by the action of external electric fields. Most of studies reported in the literature focus on microchannels or particular regions of the network, disregarding the influence of reservoirs and electrodes. Nevertheless, these elements may significantly alter the electroosmotic velocity profile, and hence sample dispersion. For instance, the connections between reservoirs and microchannels involve sudden contractions/expansions that induce pressure gradients; the electric field at the inlet/outlet of microchannels depends on the position of the electrode in the reservoir. Achieving numerical simulations of the whole microfluidic system is crucial to assist the design, control and optimization of analytical manipulations.

The most interesting aspect of computational simulation of microfluidic chips is the multiphysics nature which combines fluidics, transport, thermal, mechanics, electronics and optics with chemical, biological thermodynamics and reaction kinetics. Additionally, studying theses effects is a challenging problem from the numerical point of view. They comprise geometrical scales that span six orders of magnitude: from the millimetric size of reservoirs, passing by the micrometric width of channels, to the nanomentric thickness of the electric double layer at interfaces.

4.2 Theoretical Modeling

The foundations of electrokinetic flow are well documented in the literature [55, 56]. The case of integrated microchannel networks filled with aqueous electrolyte solutions is considered here. The electrostatic charges present at the solid-liquid interface involve an electric potential that decreases steeply in the liquid due to the screening produced by dissolved counterions and other electrolyte ions, which constitute the electric double layer.

4.2.1 Governing Equations

Electrokinetic effects arise when there is a movement of the liquid and associated ions in relation to the solid. In the framework of continuum fluid mechanics, fluid velocity $\mathbf{u}$, pressure p, and electric $\mathbf{E}$ fields are governed by the following set of coupled equations [57, 58, 59],

$$-\nabla \cdot \mathbf{u} = 0, \tag{4.1}$$

$$\rho(\frac{\partial \mathbf{u}}{\partial t} + \mathbf{u} \cdot \nabla \mathbf{u}) = \nabla \cdot \sigma + \rho \mathbf{g} + \rho_e \mathbf{E}, \tag{4.2}$$

$$\epsilon \nabla \cdot \mathbf{E} = \rho_e \, . \tag{4.3}$$

Equation 4.1 expresses the conservation of mass for incompressible fluids. Equation 4.2 (Navier–Stokes equation) expresses the conservation of momentum for Newtonian fluids of density ρ, viscosity μ, and stress tensor $\sigma = -p\mathbf{I} + \mu(\nabla \mathbf{u} + \nabla \mathbf{u}^T)$, subjected to gravitational field of acceleration $\mathbf{g}$ and electric field intensity $\mathbf{E}$. The last term on the right hand side of equation 4.2 represents the contribution of electrical forces to the momentum balance, where $\rho_e = F \sum_k z_k c_k$ is the electric charge density of the electrolyte solution, obtained as the summation over all type-k ions, with valence z_k and molar concentration c_k, and F is the Faraday constant.

Equation 4.3 (Poisson equation) establishes the relation between electric potential and charge distributions in the fluid of permittivity ϵ. Here it is relevant to mention that the ion distributions c_k (to be included in equations 4.2 and 4.3 through ρ_e must be derived from Nernst-Planck equation, which ac-

counts for the flux of type-k ions due to electrical forces, fluid convection and Brownian diffusion [56]. This coupling can be avoided by introducing a suitable simplification (see section 4.2.2).

One of the most used manipulations in microfluidic chips is electrophoretic separation of charged molecules. Thus the present work also considers the following transport equation

$$\frac{\partial c_j}{\partial t} + \mathbf{u} \cdot \nabla c_j = D_j \nabla^2 c_j - \nabla \cdot (\nu_j z_j c_j F \mathbf{E}) \,, \tag{4.4}$$

which governs the molar concentration c_j of type-j species in the electrolyte solution. In equation 4.4, D_j is the diffusion coefficient, ν_j is the mobility, and F is the Faraday constant. Therefore, once velocity u and electric field E are obtained from equations 4.1-4.3, the molar concentration profile c_j of different j species is derived from equation 4.4.

4.2.2 Electrokinetic Phenomena

Generally, most substances will acquire a surface electric charge when brought into contact with an aqueous (polar) medium. Some of the charging mechanisms include ionization, ion adsorption, and ion dissolution. The effect of any charged surface in an electrolyte solution will be to influence the distribution of nearby ions in the solution. Ions of opposite charge to that the surface (*counterions*) are attracted towards the surface while ions of like charge (*coions*) are repelled from the surface. This attraction and repulsion, when combined with the mixing tendency resulting from the random thermal motions of the ions, leads to the formation of an *electric double layer* (see figure 4.3 at page 72).

The electric double layer is a region close to the charged surface in which there is an excess of counterions over coions to neutralize the surface charge, and these ions are spatially distributed in a "diffuse" manner. Evidently there is no charge neutrality withing the double layer because the number of counterions will be large compared with the number of coions. The generated electric potentials are on the order of 50 mV. When moving away from the surface, the potential progressively decreases, and then vanishes in the liquid phase.

Electric Double Layer Theory

Consider a simple fully dissociated symmetrical salt in solution for which the number of positive and negative ions are equal, so

$$z_+ = -z_- = z\,. \tag{4.5}$$

When this electrolyte solution is brought into contact with a solid such that the surface of contact becomes positively charged, the concentrations of positive and negative ions has the following Boltzmann distribution

$$c_\pm = c_0 \exp\left(\frac{\mp zF}{RT}\phi\right)\,; \tag{4.6}$$

where ϕ is the electric potential, c_0 is the bulk salt concentration, R is the ideal gas constant and T is the absolute temperature. Clearly, the ion concentrations far from the surface $c_\pm \to c_0$ as $\phi \to 0$.

Under the above assumptions, the electric charge density is

$$\begin{aligned}\rho_e &= F\sum_k z_k c_k \\ &= F\left[+zc_0\exp\left(\frac{-zF}{RT}\phi\right) - zc_0\exp\left(\frac{+zF}{RT}\phi\right)\right] \\ &= 2zc_0F\sinh\left(-\frac{zF}{RT}\phi\right)\,;\end{aligned} \tag{4.7}$$

and the electric field $\mathbf{E}$ is related to the electric potential ϕ through

$$\mathbf{E} = -\nabla\phi\,. \tag{4.8}$$

Equations 4.7 and 4.8 can be inserted in the Poisson equation 4.3 to finally obtain

$$-\nabla^2\phi = \frac{2zc_0F}{\epsilon}\sinh\left(-\frac{zF}{RT}\phi\right). \tag{4.9}$$

The electric potential ϕ obtained through solving the Poisson–Boltzmann equation 4.9 can then be employed for determining the electric field $\mathbf{E}$ (equation 4.8) and the electric charge density ρ_e (equation 4.7). The electrical forces

can then be computed and entered in the momentum equation 4.2.

Electric Double Layer Thickness

The electric double layer thickness may be approximately quantified through the *Debye length* [55, 56],

$$\lambda_D = \sqrt{\frac{\epsilon RT}{2z^2\bar{c}F^2}}\,; \tag{4.10}$$

were $\bar{c}$ is taken to be the average molar negative ion (counterion) concentration.

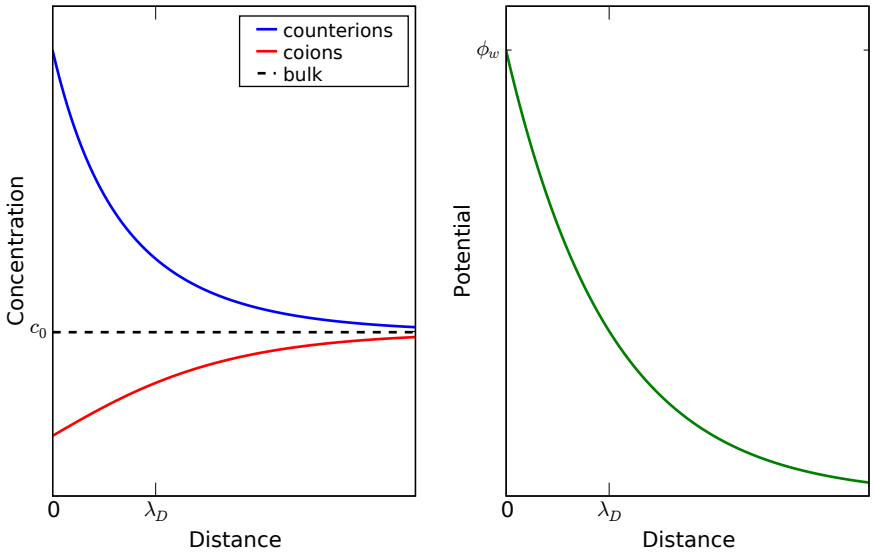

Figure 4.2: The Diffuse Double Layer and the Debye Length.

The Debye length represents the position where the electrical potential energy is approximately equal to the thermal energy of the counterions. It is obtained by neglecting the presence of coions and solving a simplified Poisson problem in the one-dimensional picture of figure 4.2.

For the ionic concentrations normally used in practice, λ_D is on the order of 10 nm. Away from the interface, at distances beyond λ_D, the bulk of the fluid is electrically neutral.

Electroosmotic Flow and Slip Velocity Approximation

Electroosmotic flow in microchannels grounds on the existence excess of ions in the fluid near solid walls. When an external electric field is applied in the axial direction of a channel, the electrical forces acting on excess ions drag the surrounding liquid and then electroosmotic flow develops.

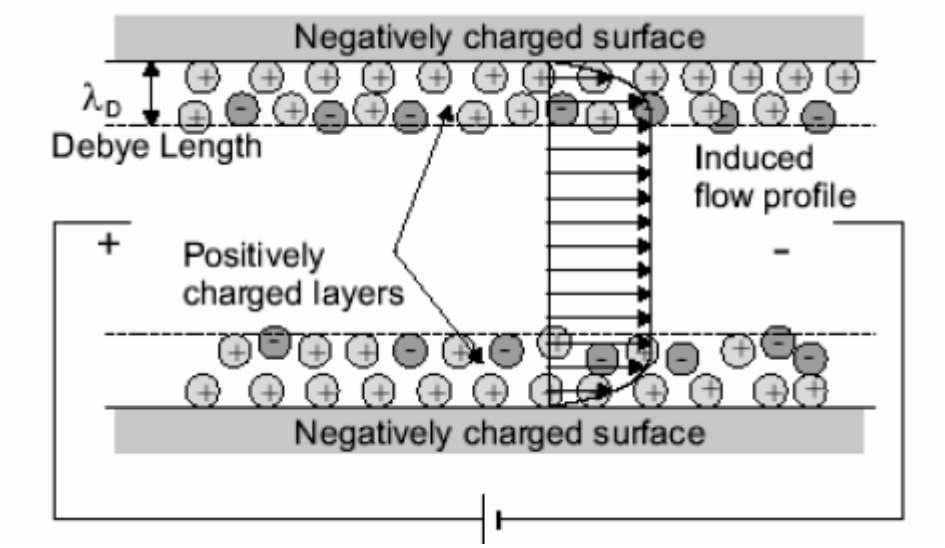

Figure 4.3: Electroosmotic Flow.

For thin electric double layer in relation to the channel width h, electroosmotic phenomena is confined to regions close to channel walls. Under these conditions, the electroosmotically driven flow can be regarded as the result of an electrically-induced *slip velocity*; its magnitude can be approximated by [55, 56]

$$\mathbf{u}_{EO} = \frac{\epsilon\zeta}{\mu}\mathbf{E}\,; \tag{4.11}$$

where ζ is the electrokinetic potential.

Further, $\mathbf{u}_{EO}$ can be used as a boundary value at the channel walls. This possibility greatly simplifies calculations since ion distributions are decoupled from Navier–Stokes and Poisson equations. In fact, if ion concentrations are assumed to be uniform (except in the close vicinity of the charged interface), and hence throughout the flow domain, the right hand side of equation 4.3 vanishes, as well as the last term of equation 4.2.

The slip velocity approximation is valid for small values of λ_D/h, which is usually the case in micro-scale channels at moderate ionic concentrations ($\approx 10^{-3}$ M). Nevertheless, at very low ionic concentrations ($\approx 10^{-6}$ M), or in case of nanoscale channels, λ_D/h approaches one, indicating that the electric double layer from opposing surfaces overlap. In that case, approximation 4.11 does not apply and the full problem must be solved.

4.3 Numerical Simulations

Previous works related to numerical simulation of electroosmotic flow and electrophoresis have restricted the problem domain to the microchannels by supposing appropriate conditions for the electric potential, velocity field, and concentrations at inlet and outlet regions. In this section, results from numerical simulations performed on a whole microfluidic system domain are presented. The influence of components like electrodes and reservoirs is investigated in order to estimate their actual significance in electroosmotic flow phenomena in general and electrophoretic separation processes in particular.

The simulations domain is a a cross-shaped microchannel network with vertical wire electrodes at reservoirs. The channel network is fabricated on a glass microscope slide with dimensions 75 mm×25 mm×1 mm. The channel sections are trapezoidal, with shape and dimensions as shown in figure 4.4.

Electrophoretic injection and separation processes are simulated in order to determine potassium and sodium ion concentrations. During the injection stage, the potentials at electrodes is selected in such a way that the intersection region is filled with a precise sample volume to be analyzed. In the separation stage, the potentials at electrodes is appropriately selected in order to achieve different relative velocities for each specie, avoiding leakages at the injection channels. The values of the relevant physical properties and constants are summarized in table 4.1.

The complete simulations requires the solution of three subsidiary problems involving charge, mass, momentum and species conservation equations described in section 4.1.

The electric fields are obtained through solving Poisson equation 4.3 (with

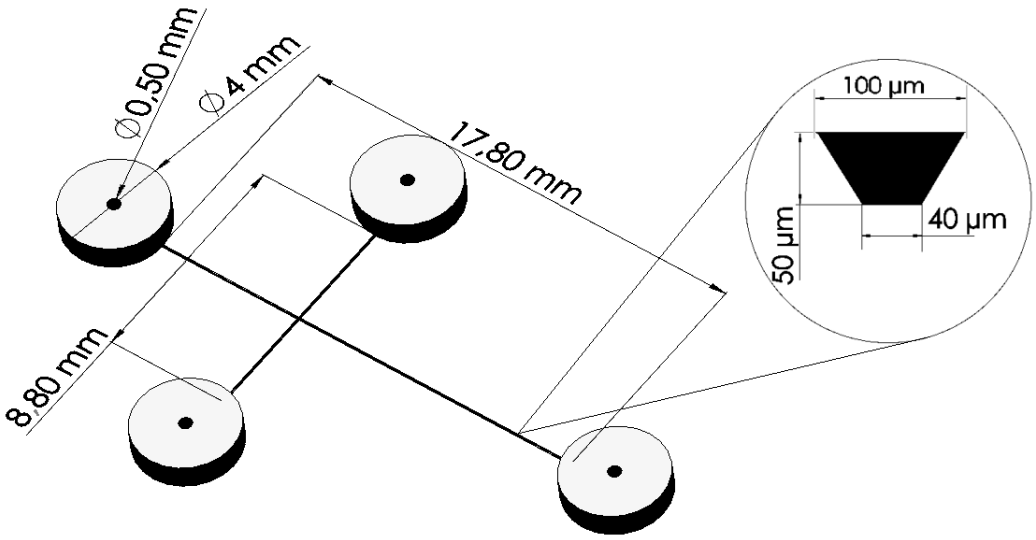

Figure 4.4: Geometry of the Microchannel Network.

Property/Constant	**Symbol**	**Value**	**Unit**
density	ρ	1000	$\mathrm{kg/m^3}$
viscosity	μ	10^{-3}	kg/m s
ionic valence	z	1	–
electrokinetic potential	ζ	$-4 \cdot 10^{-2}$	V
temperature	T	300	K
gas constant	R	8.31	J/mol K
Faraday constant	F	96485	C/mol
permittivity	ϵ	$80 \times 8.85 \cdot 10^{-12}$	F/m
sodium diffusivity	D_{Na}	$1.34 \cdot 10^{-9}$	$\mathrm{m^2/s}$
sodium mobility	ν_{Na}	$5.18 \cdot 10^{-8}$	$\mathrm{m^2/V\ s}$
potassium diffusivity	D_{K}	$1.96 \cdot 10^{-9}$	$\mathrm{m^2/s}$
potassium mobility	ν_{K}	$7.58 \cdot 10^{-8}$	$\mathrm{m^2/V\ s}$

Table 4.1: Physical Constants and Properties.

$\rho_e = 0$) for the potential and employing Dirichlet boundary conditions at electrodes and homogeneous Neumann boundary conditions at channels and reservoirs walls.

Fluid velocity is obtained by solving mass conservation equation 4.1 and Navier–Stokes equation 4.1 is stationary mode and employing as boundary condition the slip velocity approximation (equation 4.11) at the channels walls.

Finally, transport equation 4.4 is solved for the concentrations of Na^+ and Ka^+ ions by employing the electric field and fluid velocity previously obtained. This problem is transient; initial concentrations (at $t = 0$ s) are set to zero everywhere except at one of the reservoirs as shown in figure 4.5.

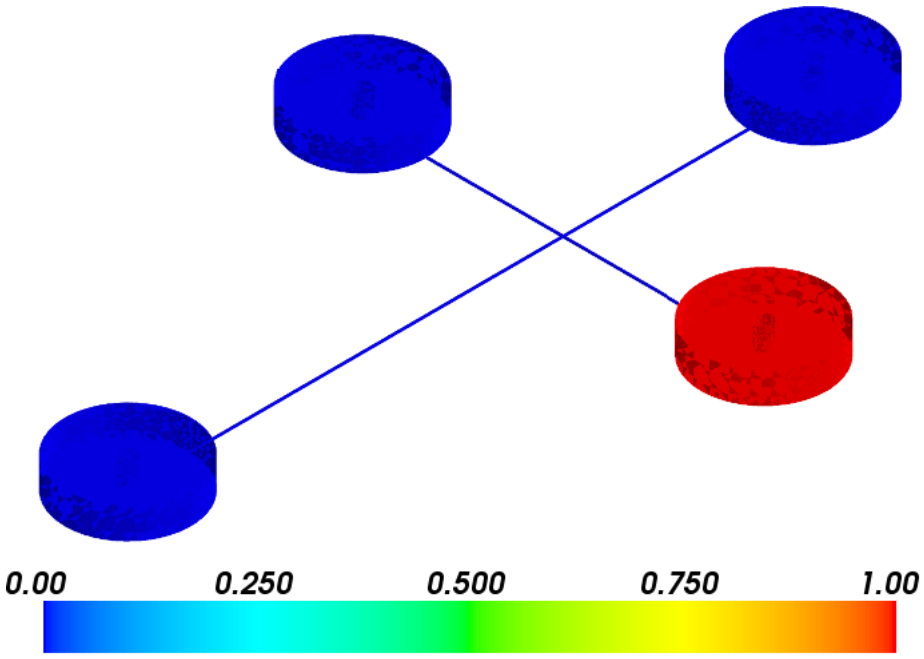

Figure 4.5: Initial Na^+ and Ka^+ Ions Concentrations (mol/m^3)

Figure 4.6 shows the applied potentials and the final (at $t = 10$ s) concentration distributions of Na^+ and Ka^+ ions during the injection stage. Figure 4.7 shows the applied potentials and concentration distributions of Na^+ and Ka^+ ions at some moment ($t = 15$ s) during the separation stage.

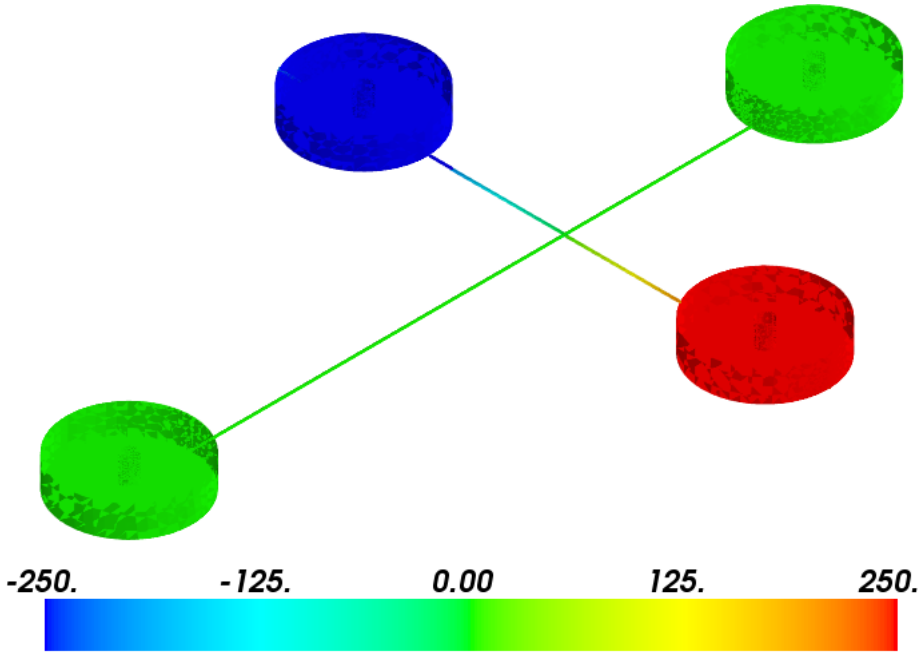

(a) applied potentials (V)

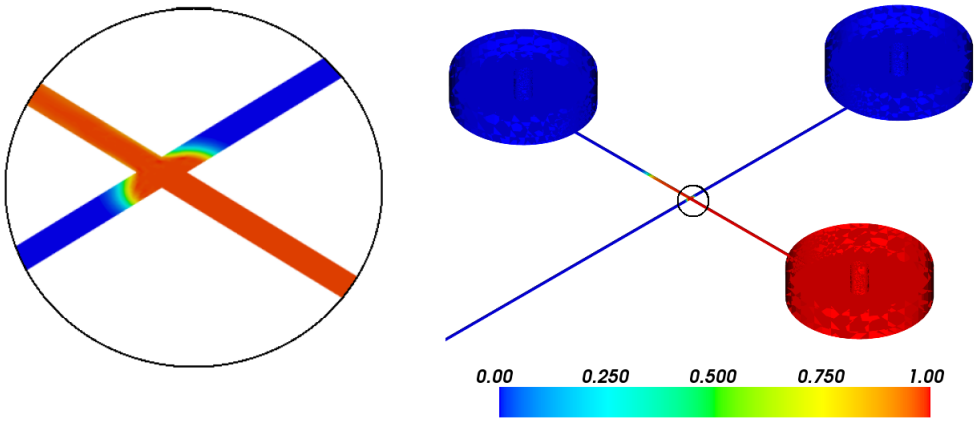

(b) ions concentrations (mol/m^3)

Figure 4.6: Injection Stage.

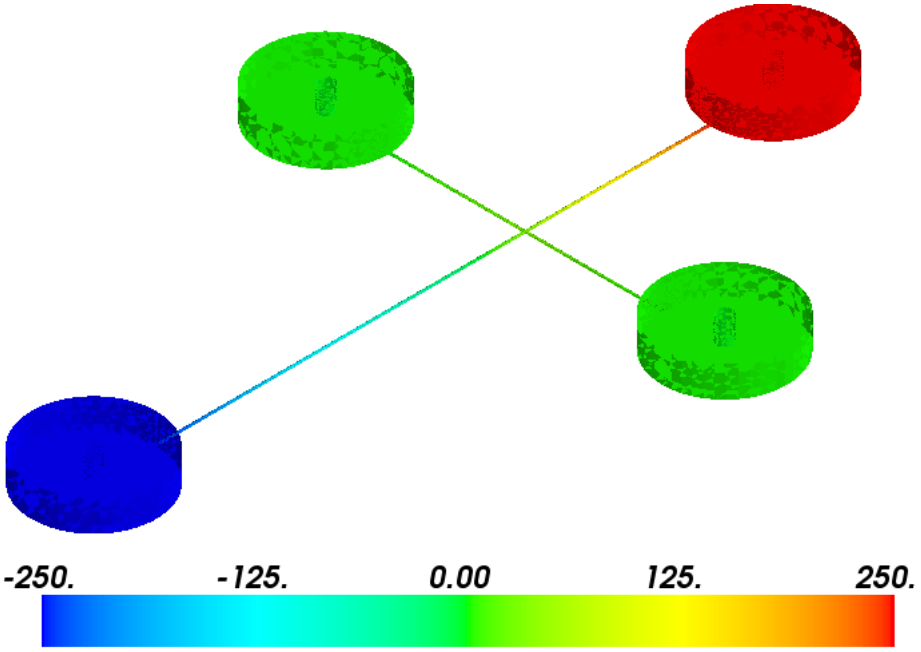

(a) applied potentials (V)

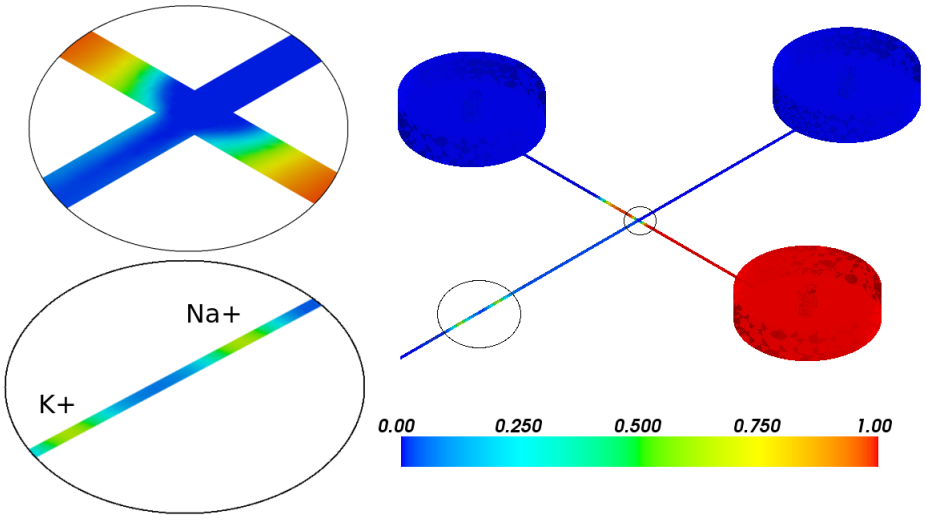

(b) ions concentrations (mol/m^3)

Figure 4.7: Separation Stage.

4.4 Classical Domain Decomposition Methods

Domain Decomposition Methods (DDM) [60] are *divide and conquer* techniques for solving boundary value problem by splitting it into smaller boundary value problems on subdomains and iterating to coordinate the solution between the subdomains. The problems on the subdomains are independent, which makes domain decomposition methods suitable for parallel computing on distributed memory architectures. Domain decomposition methods are typically used as preconditioners for Krylov space iterative methods, such as the Conjugate Gradient (CG) method or Generalized Minimal Residual (GMRES) methods.

In non-overlapping methods (also called iterative substructuring methods), the subdomains overlap only on their interface. In primal methods, such as *Balancing Domain Decomposition* (BDD) and the enhaced version BDDC [61], the continuity of the solution across subdomain interface is enforced by representing the value of the solution on all neighboring subdomains by the same unknown. In dual methods, such as *Finite Elements Tearing and Interconnecting* (FETI), the continuity of the solution across the subdomain interface is enforced by Lagrange multipliers. An enhaced, symplified and better performing version of FETI, known as FETI-DP [62], is hybrid between a dual and a primal method; its performance is essentially the same as the BDDC method. BDD and FETI mathods were primarily developed for solving of elliptic boundary value problems.

In overlapping domain decomposition methods, the subdomains overlap by more than the interface. Overlapping domain decomposition methods include the classical Schwarz alternating procedure and the *Additive Schwarz Method* (ASM) [63]. Schwarz methods can be easily applied to a variety of problems [64, 65] and can be implemented in a fully-algebraic manner (i.e. without knowledge of the underlying discrete grids).

This sections explores the applicability of additive Schwarz methods to a model problem of interest in nanoscale fluid dynamics applications.

4.4.1 A Model Problem

Consider an aqueous solution of a simple fully dissociated symmetrical salt which flows on a channel driven by the action of electrical forces originated from external electric fields. The values of the relevant physical properties and constants are summarized in the following table

Property/Constant	**Symbol**	**Value**	**Unit**
density	ρ	1000	kg/m^3
viscosity	μ	10^{-3}	kg/m s
ionic valence	z	1	–
bulk concentration	c_0	10^{-2}	mol/m^3
electrokinetic potential	ζ	$2 \cdot 10^{-2}$	V
temperature	T	300	K
gas constant	R	8.31	J/mol K
Faraday constant	F	96485	C/mol
absolute permittivity	ϵ	$80 \times 8.85 \cdot 10^{-12}$	F/m

The channel has an L-shaped geometry with an horizontal and vertical lengths of 3 μm and a cross-section of 0.4 μm × 1 μm. As the electric double layer thickness (estimated through the Debye length, equation 4.10) is around 0.1 μm, the slip velocity approximation (equation 4.11) cannot be employed.

A Laplace potential is computed by solving equation 4.3 with $\rho_e = 0$, Dirichlet boundary conditions of 0.5 V at the inlet and 0 V at the outlet, and homogeneous Neumann boundary conditions at the channel walls. A Poisson–Boltzmann potential is computed by solving the nonlinear equation 4.9 with Dirichlet boundary conditions of 20 mV (the electrokinetic potential) at the channel walls and homogeneous Neumann boundary conditions at the channel inlet and outlet. The solution for Poisson–Boltzmann potential is shown in figure 4.8b. The Laplace and Poisson–Boltzmann potentials are added-up in order to determine a total potential. Isolines of the total potential are shown in 4.8c.

Finally, Navier–Stokes equations are solved by entering the electrical forces as shown in equation 4.2. Electrical forces are determined from the total potential and Poisson–Boltzmann potential through equations 4.7 and 4.8. Non-slip

velocity boundary conditions are imposed at channel walls, and homogeneous Dirichlet boundary conditions are employed for pressure at the inlet and outlet. The computed velocity magnitude is shown in figure 4.8d.

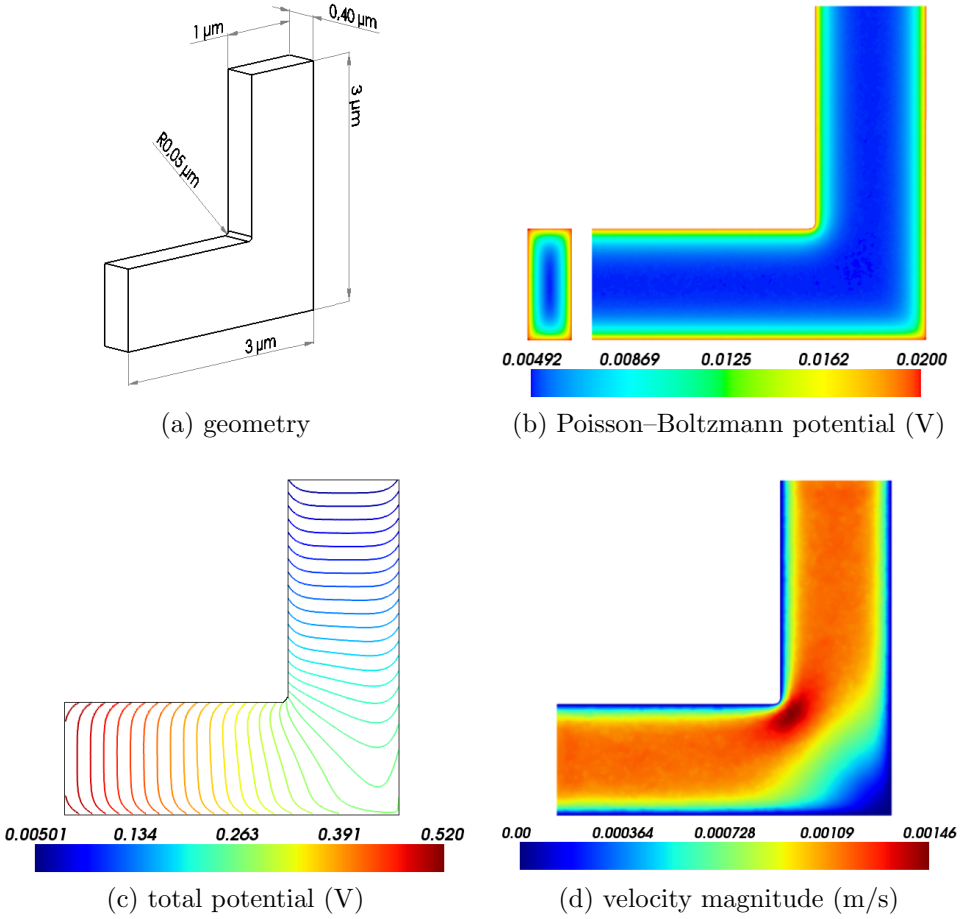

(a) geometry

(b) Poisson–Boltzmann potential (V)

(c) total potential (V)

(d) velocity magnitude (m/s)

Figure 4.8: Model Problem.

The L-shaped channel domain is discretized with three different tetrahedral meshes with increased level of refinement. The following table summarizes the number of nodes, tetrahedrons, and number of degree of freedom for the Navier–Stokes problem.

Mesh	Nodes	Elements	DOF's
#1	120,574	705,396	411,769
#2	235,011	1,406,195	828,746
#3	460,059	2,801,104	1,664,613

4.4.2 Additive Schwarz Preconditioning

The original alternating procedure described by Schwarz [66] in 1870 is an iterative method to find the solution of a partial differential equations on a domain which is the union of two overlapping subdomains, by solving the equation on each of the two subdomains in turn, taking always the latest values of the approximate solution as the boundary conditions.

The procedure described above is called the *multiplicative* Schwarz procedure. In matrix terms, this is very reminiscent of a block Gauß–Seidel iteration. The multiplicative Schwarz procedure is not fully parallel at the highest level: some processors have to wait others in order to perform the local work. The analogue of the block Jacobi procedure is known as the *additive* Schwarz procedure. The additive procedure is fully parallel; however, the convergence rate is usually slower.

The application of the additive Schwarz procedure as a preconditioning method for the solution of systems of linear equations can be summarized as follows:

1. The support mesh/grid is decomposed into N_s (possibly *overlapping*) subdomains Ω_i, $i = 1, \ldots, N_s$.

2. Each subdomain Ω_i is associated to a local space V_i with the help of a restriction operator R_i. The restriction operator R_i extract from the global vector the unknowns associated with Ω_i, while the extension operators R_i^{T} extends by zeros unknowns from Ω_i to the global vector. The preconditioner operator can then be easily written in matrix terms as

$$P^{-1} = \sum_{i=1}^{N_s} R_i^{\mathrm{T}} A_i^{-1} R_i; \tag{4.12}$$

where $A_i = R_i^{\mathrm{T}} A R_i$ are the local matrices associated with the subdomains Ω_i; they are related to the global matrix A through the restriction operators R_i. In the special case of zero overlap, the matrices A_i have entries from contributions originated in the subdomain Ω_i; if the overlap is greater than zero, the matrices A_i have additional entries contributed by neighboring subdomains.

3. Any Krylov-based iterative method can then be employed for solving the (left) preconditioned linear system $P^{-1}Ax = P^{-1}b$.

Many factors impact the performance of additive Schwarz preconditioning in the context of parallel iterative methods for the solution of systems of linear equations. The main ones are summarized in the following list.

- Additive Schwarz methods are normally implemented in such a way that the number of subdomains N_s and the restriction operators R_i are inherited from the previous partitioning of the underlying discrete grid or mesh. The local problems (involving matrix A_i in equation 4.12) are usually solved by variants of incomplete factorization methods (e.g. ILU(0)). For well-conditioned problems, incomplete factorization methods are the faster alternative regarding to overall wall-clock computing time.

- Iterative methods frequently stagnate when then global problem is ill-conditioned and the local problems are treated with incomplete factorizations. In such cases, the local problems have to be solved either with and inner iterative method or a full direct method (i.e. LU factorization). In either case, as the size of the local subdomain increases, also do the time required for obtaining the local solution. This is specially true when the local solver is based on a LU factorization. In order to employ a direct method and maintaining the size of local problems manageable, local subdomains can be further partitioned at each processor in sub-subdomains. This strategy degrades convergence, but can improve the overall solution time.

- As the overlap increases, convergence rate improves; but computing, communication and memory requirements increase. Ghost vector val-

ues have to be gathered from and scattered to neighboring processors at each iteration; matrix values have to be gathered from neighboring processors in a setup phase, and the local problems to solve are larger (in the setup-phase factorization as well as in the backward/forward solves at each iteration). Then, as overlap increases, actual improvements in the total wall-clock time for obtaining the final solution will depend upon the balance between better convergence rates versus the extra costs.

- Finally, for global problems of medium to large scale, as the number of processors assigned to its solution increases, the parallel efficiency decreases. Actually, this behavior is shared for any non-embarrassingly parallel algorithm. As a rule of thumb, each processor have to be in charge of 50,000 to 100,000 unknowns (depending on computing and network hardware) to achieve parallel speedup.

The rest of this subsection explores the issues commented previously by applying the additive Schwarz preconditioner to the model problem on the three discretizations described in subsection 4.4.1.

Although the problem at hand is essentially linear, it is solved as a full nonlinear one employing two iteration of a standard Newton method. In all the test cases, the final (outer, nonlinear) residual norm is reduced by a factor of around 10^{-6}.

The linear systems at each nonlinear step are solved with GMRES(250) (i.e. GMRES restarted at 250 iterations) by defining a fixed relative tolerance of 10^{-4} for the reduction of the initial (inner, linear) residual norm.

The additive Schwarz method is employed as a left-preconditioner within GMRES iterations. Being the global linear systems of saddle-point nature, they are ill-conditioned. Incomplete factorizations methods cannot be practically employed for the local problems, as this leads to GMRES stagnation. Thus, the local problems are solved by employing full direct methods and aggressive subdomain sub-partitioning at each processor. The sub-partitioning is performed on the adjacency graph obtained from the local, *diagonal* part of the global sparse matrix with the help of METIS [67] library.

In all test cases discussed below, wall-clock time measurements do not account for the time required for evaluating and assembling residual vectors and Jacobian matrices, but only for the time spent in solving the linear systems. Parallel efficiency is computed by taking as reference the timings of the runs performed on the smaller number of processes, i.e. $E_p = (P_{\min} T_{P_{\min}})/(pT_p)$, where $p = \{P_{\min}, \ldots, P_{\max}\}$ is the set of number of processes employed and T_p is the wall-clock time measurement with p processes.

Figures 4.9 to 4.11 shows wall-clock time measurements and parallel efficiency for the additive Schwarz preconditioner with overlap zero. The model problem is solved on the meshes #1, #2, and #3 employing 20, 30, 40, and 50 processors. The subdomain sizes range from 1000 to 4000 unknowns. For meshes #1 and #2, a subdomain size of around 1000 unknowns seems to be optimal, while for mesh #3, the optimal subdomain size is around 2500 unknowns. Clearly, depending on the problem size, as the number of processors increase beyond some limit the required wall-clock time for obtaining the solution do not decrease but stagnates.

Remarkably, figure 4.10 shows that for the case of mesh #2, the solution times are almost the same on 40 and 50 processors. Similarly, figure 4.11 shows that for the case of mesh #3, the solution times are almost the same on 30, 40, and 50 processors. Figure 4.12 shows wall-clock time measurements and parallel efficiency for the case of mesh #3 only on 16, 24, and 32 processors and a broader range of subdomain sizes.

Finally, figure 4.13 shows wall-clock time measurements for the additive Schwarz preconditioner with overlap zero and one. Clearly, increasing the overlap also increases the solution time.

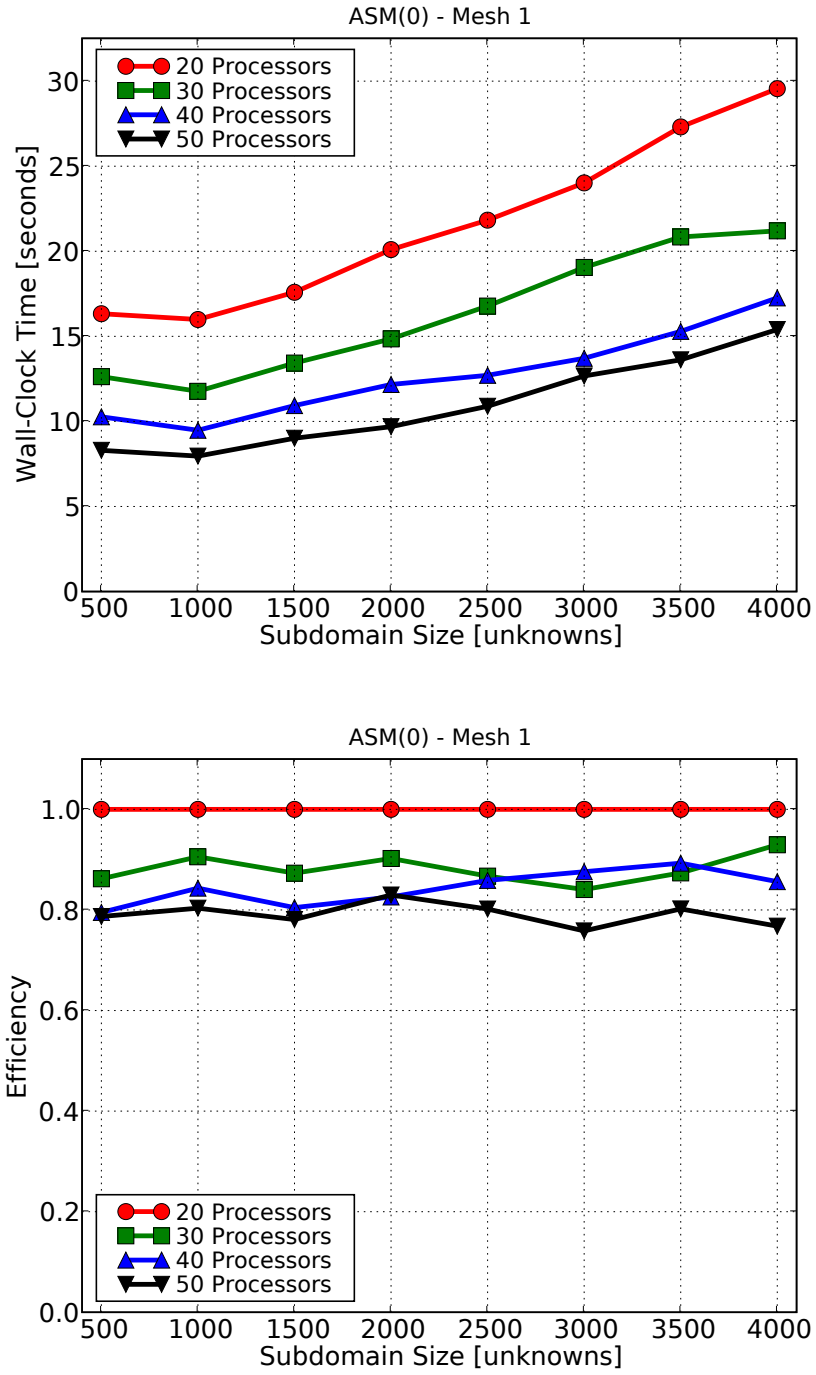

Figure 4.9: Additive Schwarz Preconditioning (Mesh #1).

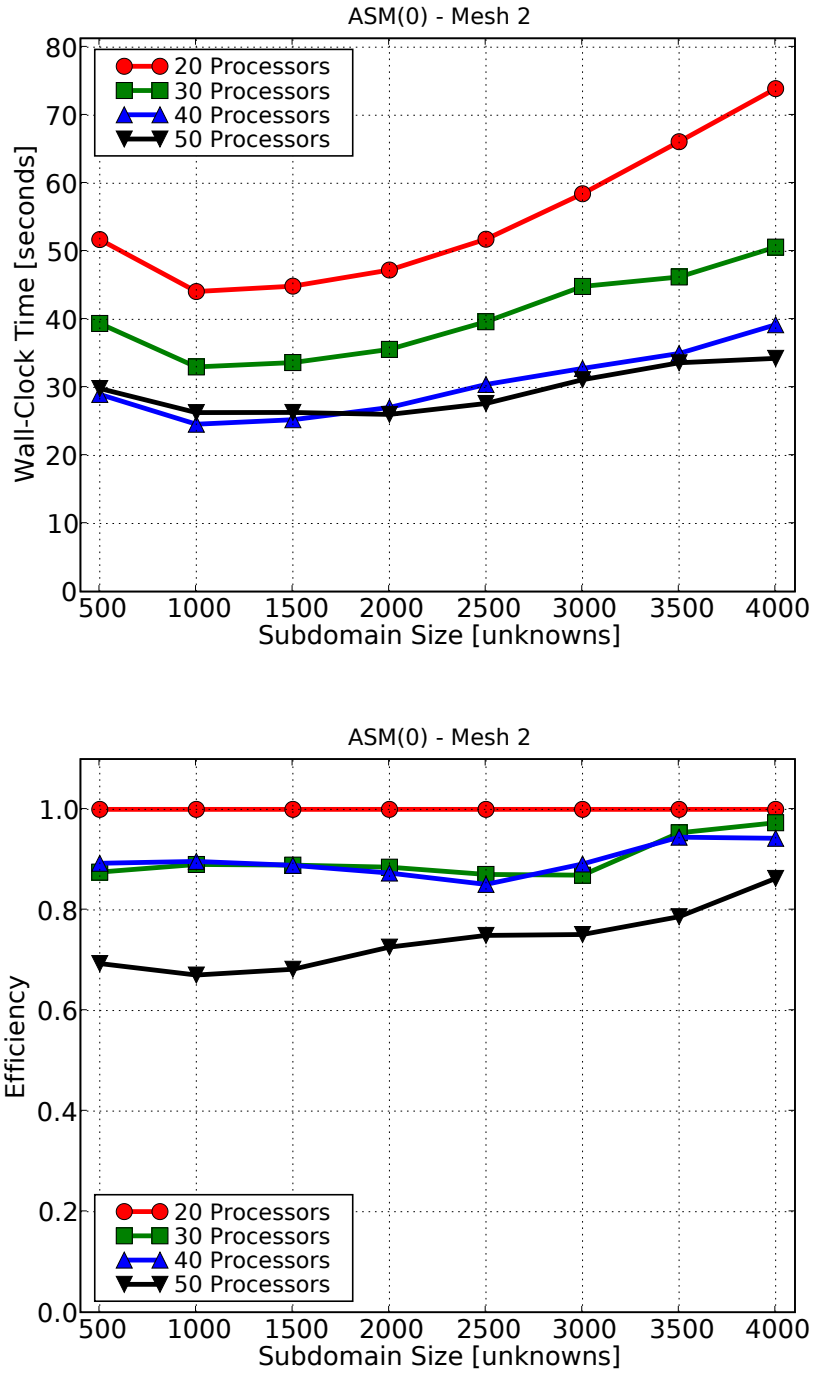

Figure 4.10: Additive Schwarz Preconditioning (Mesh #2).

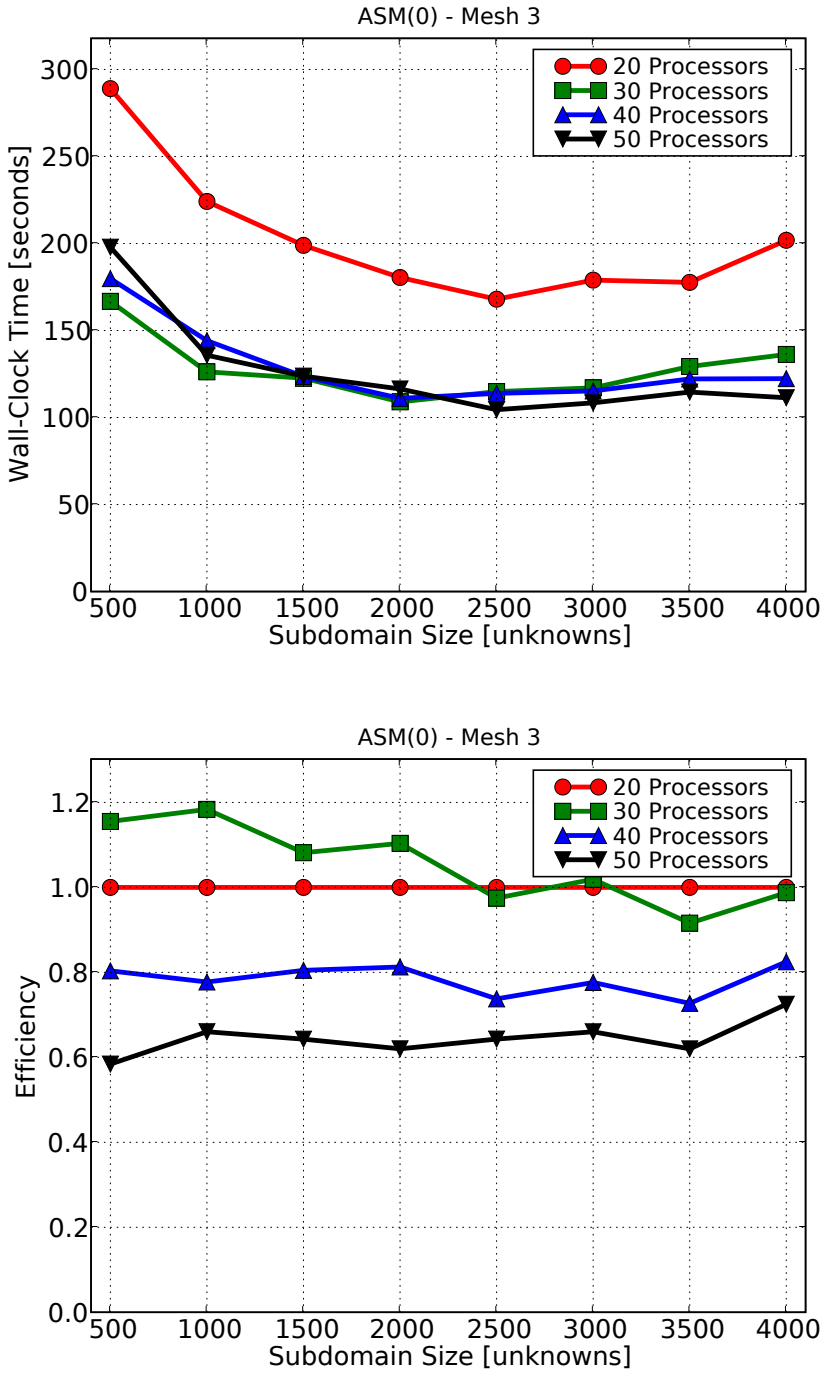

Figure 4.11: Additive Schwarz Preconditioning (Mesh #3).

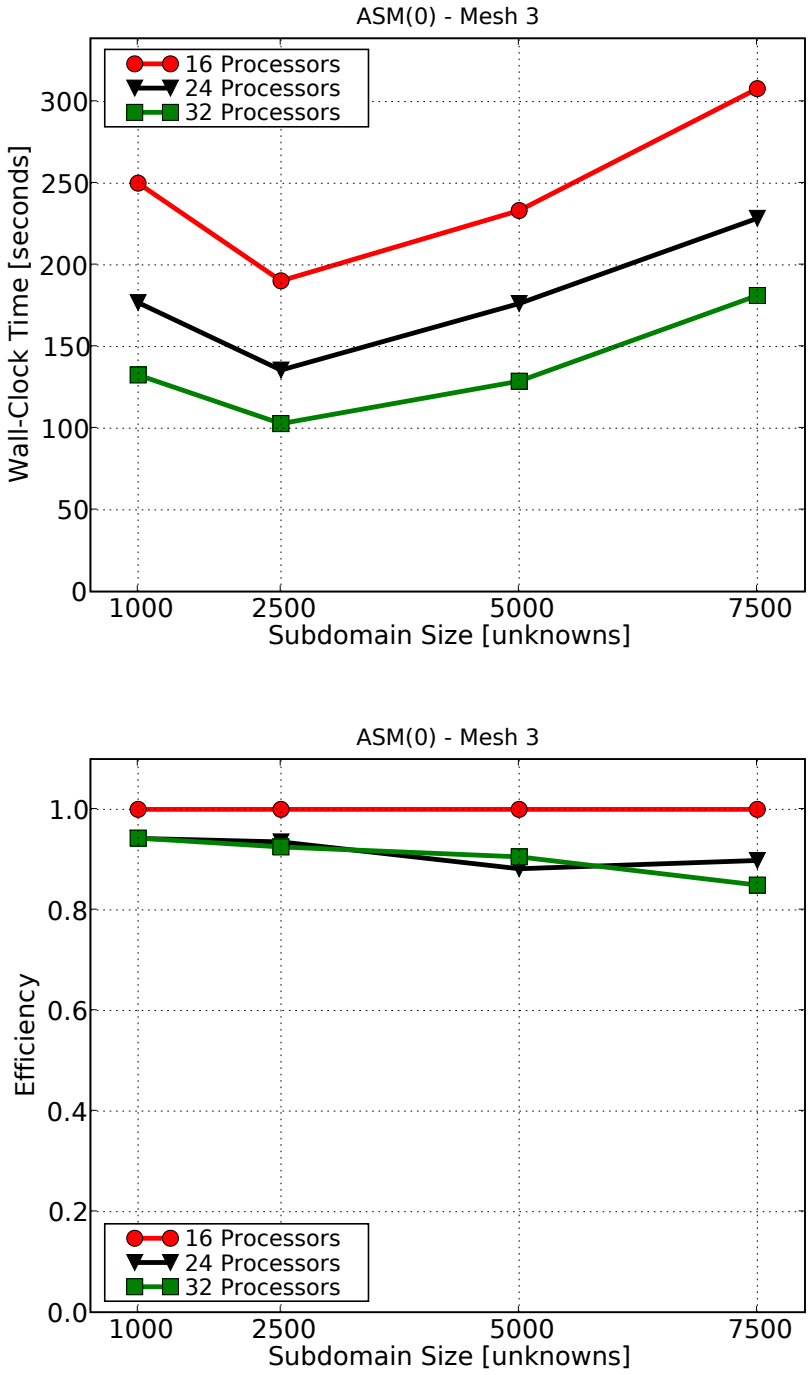

Figure 4.12: Additive Schwarz Preconditioning (Mesh #3).

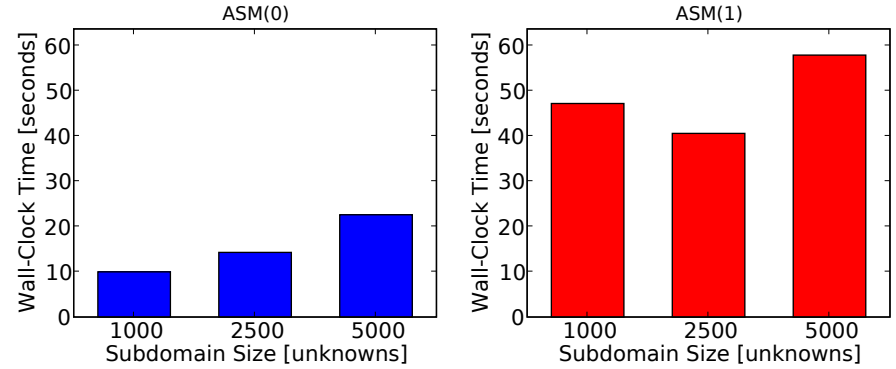

(a) Mesh #1

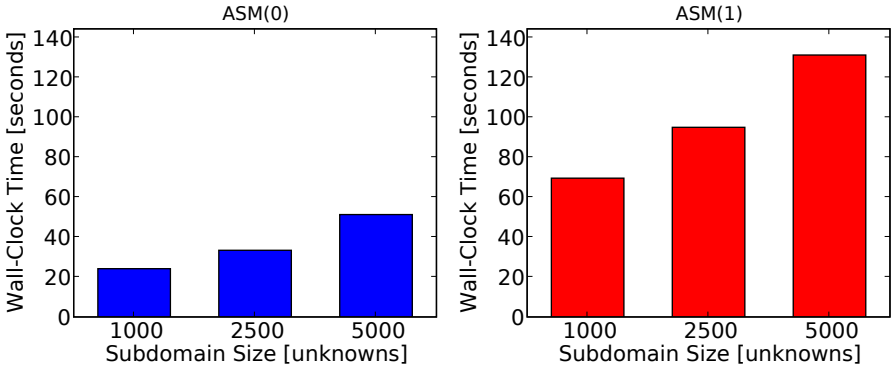

(b) Mesh #2

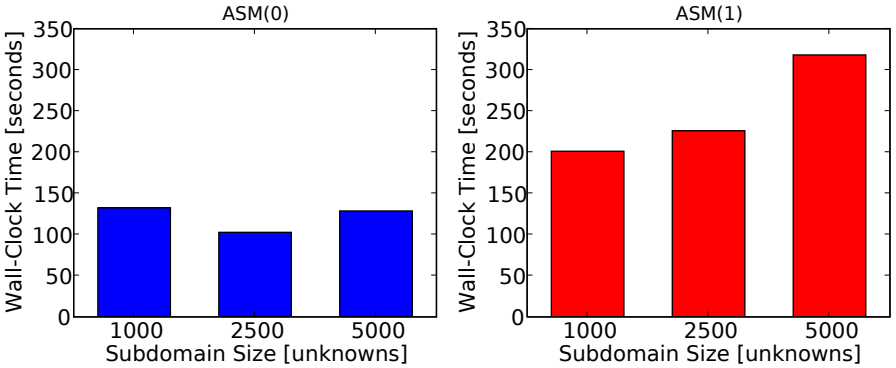

(c) Mesh #3

Figure 4.13: Additive Schwarz Preconditioning (32 processors).

Chapter 5

Final Remarks

5.1 Impact of this work

MPI for Python and PETSc for Python were primarily conceived to be small packages providing very basic parallel functionalities. The original intention revolved around providing a programmable scripting interface to *PETSc-FEM*. As time passed, MPI for Python and PETSc for Python progressively evolved and gained more and more functionalities. At the time of this writing, they had become full-featured packages able to support serious medium and large scale parallel applications.

MPI for Python and PETSc for Python are serving the original purposes that initially motivated their development. Currently, both packages are fully integrated to a Python module providing access to *PETSc-FEM* functionalities. However, the initial intent of providing *PETSc-FEM* with a programmable scripting interface was early abandoned. Using *PETSc-FEM* functionalities directly from a Python programming environment is a much more attractive and productive alternative. Python codes are being used for driving *PETSc-FEM* parallel finite elements simulations. This software infraestructure is supporting research activities related to fluid flow in micro-channels, fluid-structure interaction, and fluid-induced vibration.

The *Synergia 3D* project [68] is developed by the Advanced Accelerator Modelling team at the Fermilab Computing Division. The software simulates

the behavior of particles in an accelerator, emphasizing three-dimensional models of collective beam effects. This project uses Python-driven Fortran 90 and C++ libraries to create beam dynamics simulations. The individual beam dynamics libraries were designed to use MPI to support parallel computation. MPI for Python is used from the Python-driven simulations to support communication within MPI at the Python level.

MPI for Python has also been successfully employed in non-scientific applications. The *Ghostscript* project, a well-known and widely used interpreter for the *PostScript* language, has taken advantage of MPI for Python for moving its originally sequential and Python-based software regression testing framework–targeted to early detect unintended behavior changes during development–to a traditional cluster-based environment. Originally, the huge test suite took hours to complete. After parallelization, the automated checks could be performed after every source code change, returning feedback in a few minutes. MPI for Python was chosen because it provided the best mix of the traditional MPI features developers were familiar to and its integration with the Python language.

Some core component of PETSc for Python have recently served as the foundation for further developments. SLEPc for Python [69] (known in short as *slepc4py*) is a recent software project providing access to to the *Scalable Library for Eigenvalue Problem Computations* (SLEPc) [70, 71] for the Python programming language. SLEPc is a software library for the solution of large scale sparse eigenvalue problems on parallel computers; it is being developed by the High Performance Networking and Computing Group of the Universidad Politécnica de Valencia, Spain. SLEPc for Python is being developed at the University of Nebraska-Lincoln, USA. The core developers of SLEPc and the author of this thesis have also colaborated and made contributions to it.

5.2 Publications

During the work on this thesis the following articles have been published or are going to be published in referred journals.

1. **Alejandro Limache, Pablo Sánchez, Lisandro D. Dalcín, and Sergio Idelsohn**. Objectivity tests for Navier-Stokes simulations: the revealing of non-physical solutions produced by Laplace formulations. *Computer Methods in Applied Mechanics and Engineering*, In Press, 2008. doi:10.1016/j.cma.2008.04.020

2. **Lisandro D. Dalcín, Rodrigo R. Paz and Mario A. Storti**. MPI for Python: performance improvements and MPI-2 extensions. *Journal of Parallel and Distributed Computing*, **68(5)**:655-662, 2008. doi:10.1016/j.jpdc.2007.09.005

3. **Mario A. Storti, Norberto M. Nigro, Rodrigo R. Paz and Lisandro D. Dalcín**. Dynamics boundary conditions in fluid mechanics. *Computer Methods in Applied Mechanics and Engineering*, **197(13-16)**:1219-1232, 2008. doi:10.1016/j.cma.2007.10.014

4. **Mario A. Storti, Lisandro D. Dalcín, Rodrigo R. Paz, Andrea Yommi, Victorio Sonzogni, and Norberto M. Nigro**. A preconditioner for the Schur complement matrix. *Advances in Engineering Software*, **37(11)**:754-762, 2006. doi:10.1016/j.advengsoft.2006.02.003

5. **Lisandro D. Dalcín, Rodrigo R. Paz and Mario A. Storti**. MPI for Python. *Journal of Parallel and Distributed Computing*, **65(9)**:1108-1115, 2005. doi:10.1016/j.jpdc.2005.03.010

Additionally, several articles have been submitted and presented in national international conferences at Argentina on numerical methods for computational mechanics.

Bibliography

[1] Beowulf.org. The Beowulf cluster site, 2008. `http://www.beowulf.org/`. ix

[2] Satish Balay, Kris Buschelman, William D. Gropp, Dinesh Kaushik, Matthew G. Knepley, Lois Curfman McInnes, Barry F. Smith, and Hong Zhang. PETSc Web page, 2008. `http://www.mcs.anl.gov/petsc`. x, 40

[3] The Trilinos Team Sandia National Laboratories. The Trilinos project, 2008. `http://trilinos.sandia.gov`. x

[4] Satish Balay, Kris Buschelman, Victor Eijkhout, William D. Gropp, Dinesh Kaushik, Matthew G. Knepley, Lois Curfman McInnes, Barry F. Smith, and Hong Zhang. PETSc users manual. Technical Report ANL-95/11 - Revision 2.3.3, Argonne National Laboratory, 2007. x, 40

[5] Satish Balay, William D. Gropp, Lois Curfman McInnes, and Barry F. Smith. Efficient management of parallelism in object oriented numerical software libraries. In E. Arge, A. M. Bruaset, and H. P. Langtangen, editors, *Modern Software Tools in Scientific Computing*, pages 163–202. Birkhäuser Press, 1997. x, 40

[6] Guido van Rossum. Python programming language, 1990–2008. `http://www.python.org/`. x, 1

[7] Guido van Rossum. Python reference manual. `http://docs.python.org/ref/ref.html`, May 2008. x

[8] Lisandro Dalcín, Rodrigo Paz, and Mario Storti. MPI for Python. *Journal of Parallel and Distributed Computing*, 65(9):1108–1115, sep 2005. xii

[9] Lisandro Dalcín, Rodrigo Paz, and Mario Storti Jorge D'Elia. MPI for Python: Performance improvements and MPI-2 extensions. *Journal of Parallel and Distributed Computing*, 68(5):655–662, may 2008. xii

[10] Lisandro Dalcín. MPI for Python, 2005-2008. `http://mpi4py.scipy.org`. xii

[11] Lisandro Dalcín. PETSc for Python, 2005-2008. `http://petsc4py.googlecode.com/`. xii

[12] Mario Alberto Storti, Norberto Nigro, and Rodrigo Paz. PETSc-FEM: A general purpose, parallel, multi-physics FEM program, 1999-2008. `http://www.cimec.org.ar/petscfem`. xii, 65

[13] Travis Oliphant. NumPy: Numerical Python, 2005–2008. `http://numpy.scipy.org/`. 2

[14] Eric Jones, Travis Oliphant, Pearu Peterson, et al. SciPy: Open source scientific tools for Python, 2001–2008. `http://www.scipy.org/`. 2

[15] Pearu Peterson. F2PY: Fortran to Python interface generator, 2000–2008. `http://cens.ioc.ee/projects/f2py2e/`. 2

[16] David M. Beazley. SWIG: Simplified wrapper and interface generator, 1996–2008. `http://www.swig.org/`. 3

[17] David M. Beazley and Peter S. Lomdahl. Feeding a large scale physics application to Python. In *Proceedings of 6th. International Python Conference*, pages 21–29, San Jose, California, October 1997. 3

[18] K. Kadau, T. C. Germann, and P. S. Lomdahl. Molecular Dynamics Comes of Age:. 320 Billion Atom Simulation on BlueGene/L. *International Journal of Modern Physics C*, 17:1755–1761, 2006. 3

[19] Marc Snir, Steve Otto, Steven Huss-Lederman, David Walker, and Jack Dongarra. *MPI - The Complete Reference: Volume 1, The MPI Core*, volume 1, The MPI Core. MIT Press, Cambridge, MA, USA, 2nd. edition, 1998. 6

[20] William Gropp, Steven Huss-Lederman, Andrew Lumsdaine, Ewing Lusk, Bill Nitzberg, William Saphir, and Marc Snir. *MPI - The Complete Reference: Volume 2, The MPI-2 Extensions*, volume 2, The MPI-2 Extensions. MIT Press, Cambridge, MA, USA, 2nd. edition, 1998. 6

[21] Message Passing Interface Forum. Message Passing Interface (MPI) Forum Home Page, 2008. `http://www.mpi-forum.org/`. 7

[22] MPI Forum. MPI: A message passing interface standard. *International Journal of Supercomputer Applications*, 8(3/4):159–416, 1994. 7

[23] MPI Forum. MPI2: A message passing interface standard. *High Performance Computing Applications*, 12(1–2):1–299, 1998. 7

[24] MPICH Team. MPICH: A portable implementation of MPI, 2005. `http://www-unix.mcs.anl.gov/mpi/mpich/`. 7

[25] W. Gropp, E. Lusk, N. Doss, and A. Skjellum. A high-performance, portable implementation of the MPI message passing interface standard. *Parallel Computing*, 22(6):789–828, September 1996. 7

[26] Open MPI Team. Open MPI: Open source high performance computing, 2008. `http://www.open-mpi.org/`. 7

[27] Edgar Gabriel, Graham E. Fagg, George Bosilca, Thara Angskun, Jack J. Dongarra, Jeffrey M. Squyres, Vishal Sahay, Prabhanjan Kambadur, Brian Barrett, Andrew Lumsdaine, Ralph H. Castain, David J. Daniel, Richard L. Graham, and Timothy S. Woodall. Open MPI: Goals, concept, and design of a next generation MPI implementation. In *Proceedings, 11th European PVM/MPI Users' Group Meeting*, pages 97–104, Budapest, Hungary, September 2004. 7

[28] Institute of Electrical and Electronics Engineers. *System Application Program Interface (API) [C Language].* Information technology—Portable Operating System Interface (POSIX). IEEE Computer Society, 345 E. 47th St, New York, NY 10017, USA, 1990. 11

[29] Jeffrey M. Squyres, Jeremiah Willcock, Brian C. McCandless, Peter W. Rijks, and Andrew Lumsdaine. OOMPI Home page, 1996. `http://www.osl.iu.edu/research/oompi/`. 11

[30] Brian C. McCandless, Jeffrey M. Squyres, and Andrew Lumsdaine. Object oriented MPI (oompi): a class library for the message passing interface. In *MPI Developer's Conference*, pages 87–94, Jul 1996. 11

[31] Patrick Miller. pyMPI: Putting the py in MPI, 2000–2008. `http://pympi.sourceforge.net/`. 12

[32] Ole Nielsen. Pypar Home page, 2002–2008. `http://datamining.anu.edu.au/~ole/pypar/`. 12

[33] Konrad Hinsen. ScientificPython: Home page, 2008. `http://dirac.cnrs-orleans.fr/plone/software/scientificpython/`. 12

[34] Mario Alberto Storti. Aquiles cluster at CIMEC, 2005-2008. `http://www.cimec.org.ar/aquiles`. 28, 58

[35] Mario Alberto Storti. Geronimo cluster at CIMEC, 2001–2005. `http://www.cimec.org.ar/geronimo`. 35

[36] R.D. Falgout, J.E. Jones, and U.M. Yang. *Numerical Solution of Partial Differential Equations on Parallel Computers*, volume 51, chapter The Design and Implementation of hypre, a Library of Parallel High Performance Preconditioners, pages 267–294. Springer-Verlag, 2006. 41

[37] Michael Heroux, Roscoe Bartlett, Vicki Howle Robert Hoekstra, Jonathan Hu, Tamara Kolda, Richard Lehoucq, Kevin Long, Roger Pawlowski, Eric Phipps, Andrew Salinger, Heidi Thornquist, Ray Tuminaro, James Willenbring, and Alan Williams. An Overview of Trilinos. Technical Report SAND2003-2927, Sandia National Laboratories, 2003. 41

[38] P. R. Amestoy, I. S. Duff, J.-Y. L'Excellent, and J. Koster. A fully asynchronous multifrontal solver using distributed dynamic scheduling. *SIAM Journal on Matrix Analysis and Applications*, 23(1):15–41, 2001. 41

[39] Steven Bernard and Marcus Grote. SPAI Web Page. `http://www.sam.math.ethz.ch/~{}grote/spai/`. 41

[40] Peter N. Brown and Youcef Saad. Hybrid Krylov methods for nonlinear systems of equations. *SIAM J. Sci. Stat. Comput.*, 11:450–481, 1990. 44

[41] M. Pernice and H. F. Walker. NITSOL: A Newton iterative solver for nonlinear systems. *SIAM J. Sci. Stat. Comput.*, 19:302–318, 1998. 44

[42] R. Barrett, M. Berry, T. F. Chan, J. Demmel, J. Donato, J. Dongarra, V. Eijkhout, R. Pozo, C. Romine, and H. Van der Vorst. *Templates for the Solution of Linear Systems: Building Blocks for Iterative Methods, 2nd Edition.* SIAM, Philadelphia, PA, 1994. 55

[43] Victorio E. Sonzogni, Andrea M. Yommi, Norberto M. Nigro, and Mario A. Storti. A parallel finite element program on a Beowulf cluster. *Advances in Engineering Software*, 33(7–10):427–443, July / October 2002. 65

[44] T. Tezduyar, S. Mittal, S. Ray, and R. Shih. Incompressible flow computations with stabilized bilinear and linear equal order interpolation velocity pressure elements. *Computer Methods in Applied Mechanics and Engineering*, 95:221–242, 1992. 66

[45] T.E. Tezduyar and Y. Osawa. Finite element stabilization parameters computed from element matrices and vectors. *Computer Methods in Applied Mechanics and Engineering*, 190(3-4):411–430, 2000. 66

[46] D.R. Reyes, D. Iossifidis, P.A. Auroux, and A. Manz. Micro total analysis systems. 1. introduction, theory, and technology. *Analytical Chemistry*, 74(12):2623–2636, 2002. 66

[47] M. Freemantle. Downsizing chemistry: Chemical analysis and synthesis on microchips promise a variety of potential benefits. *Chemical Engineering News*, 77:27–36, 1999. 66

[48] M.J. Madou. *Fundamentals of Microfabrication: The Science of Miniaturization.* CRC Press, second edition, 2002. 66

[49] D. Erickson and D. Li. Integrated microfluidic devices. *Analytica Chimica Acta*, 507(1):11–26, 2004. 67

[50] N.A. Patankar and H.H. Hu. Numerical simulation of electroosmotic flow. *Analytical Chemistry*, 70(9):1870–1881, 1998. 67

[51] F. Bianchi, R. Ferrigno, and H.H. Girault. Finite element simulation of an electroosmotic-driven flow division at a t-junction of microscale dimensions. *Analytical Chemistry*, 72(9):1987–1993, 2000. 67

[52] N. Sundararajan, M.S. Pio, L.P. Lee, and A.A. Berlin. Three-dimensional hydrodynamic focusing in polydimethylsiloxane (pdms) microchannels. *Journal of Microelectromechanical Systems*, 13(4):559–567, 2004. 67

[53] J.M. MacInnes, X. Du, and R.W.K. Allen. Prediction of electrokinetic and pressure flow in a microchannel T-junction. *Physics of Fluids*, 15(7):1992–2005, 2003. 67

[54] D. Erickson. Towards numerical prototyping of labs-on-chip: modeling for integrated microfluidic devices. *Microfluidics and Nanofluidics*, 1(4):301–318, 2005. 67

[55] Hunter R.J. *Foundations of Colloid Science*. Oxford University Press, second edition, 2001. 68, 71, 72

[56] Probstein R.F. *Physicochemical Hydrodynamics. An Introduction*. Wiley-Interscience, second edition, 2003. 68, 69, 71, 72

[57] P. Tabeling. *Introduction to Microfluidics*. Oxford University Press, 2005. 68

[58] Stone H.A., Stroock A.D., and Ajdari A. Engineering flows in small devices: Microfluidics toward a lab-on-a-chip. *Annual Review of Fluid Mechanics*, 36:381–411, 2004. 68

[59] T.M. Squires and S.R. Quake. Microfluidics: Fluid physics at the nanoliter scale. *Reviews of Modern Physics*, 77(3), 2005. 68

[60] Barry F. Smith, Petter E. Bjørstad, and William Gropp. *Domain Decomposition: Parallel Multilevel Methods for Elliptic Partial Differential Equations*. Cambridge University Press, 1996. 78

[61] Clark R. Dohrmann. A preconditioner for substructuring based on constrained energy minimization. *SIAM Journal on Scientific Computing*, 25(1):246–258, 2003. 78

[62] Charbel Farhat, Michel Lesoinne, Patrick LeTallec, Kendall Pierson, and Daniel Rixen. FETI-DP: a dual-primal unified FETI method - part i: A faster alternative to the two-level FETI method. *International Journal for Numerical Methods in Engineering*, 50(7):1523–1544, 2001. 78

[63] Andreas Frommer and Hartmut Schwandt. A unified representation and theory of algebraic additive Schwarz and multisplitting methods. *SIAM J. Matrix Anal. Appl.*, 18(4):893–912, 1997. 78

[64] Martin J. Gander and Laurence Halpern. Optimized Schwarz waveform relaxation methods for advection reaction diffusion problems. *SIAM J. Numer. Anal.*, 45(2):666–697, 2007. 78

[65] Martin J. Gander, Laurence Halpern, and Frédéric Magoulès. An optimized schwarz method with two-sided robin transmission conditions for the helmholtz equation. *International. Journal for Numerical Methods in Fluids*, 55(2):163–175, 2007. 78

[66] Hermann. A. Schwarz. Über einen Grenzübergang durch alternierendes Verfahren. *Vierteljahrsschrift der Naturforschenden Gesellschaft in Zürich*, 15:272–286, May 1870. 81

[67] George Karypis and Vipin Kumar. Multilevel k-way partitioning scheme for irregular graphs. *Journal of Parallel and Distributed Computing*, 48(1):96–129, 1998. 83

[68] J. Amundson, P. Spentzouris, J. Qiang, and R. Ryne. Synergia: A 3D accelerator modelling tool with 3D space charge. *Journal of Computational Physics*, 211(1):229–248, January 2006. 91

[69] Brian Bockelman. SLEPc for Python, 2008. `http://t2.unl.edu/documentation/slepc4py`. 92

[70] Vicente Hernandez, Jose E. Roman, and Vicente Vidal. SLEPc: A scalable and flexible toolkit for the solution of eigenvalue problems. *ACM Transactions on Mathematical Software*, 31(3):351–362, September 2005. 92

[71] Vicente Hernandez, Jose E. Roman, and Vicente Vidal. SLEPc Web page, 2008. `http://www.grycap.upv.es/slepc/`. 92